Atmos. Chem. Phys. Discuss.,
https://doi.org/10.5194/acp-2019-620-AC1, 2019

Atmospheric Chemistry and Physics Discussions

Interactive comment on "Experimental investigation into the volatilities of highly oxygenated organic molecules (HOM)" *by* Otso Peräkylä et al.

Otso Peräkylä et al.

otso.perakyla@helsinki.fi

Received and published: 26 October 2019

We thank the two anonymous reviewers for the insightful and constructive comments and questions regarding our manuscript. We have addressed the reviewers' comments point-by-point below:

1 Anonymous Referee 1

This manuscript presents an experimental investigation of the volatilities of highly oxygenated organic compounds (HOM) formed in the ozonolysis of α-pinene. The condensation behaviors of HOM upon seed injection in continuous flow chamber experiments were interpreted using box modelling to offer insights into their volatilities. The authors found that HOM dimers, along with the majority of HOM monomers are of low or extremely low volatility, while a small fraction of HOM monomers are semi-volatile. The authors further developed a parameterization for assessing the volatilities of HOM using their molecular composition, and compared the results with those derived by existing volatility parameterizations. This manuscript provides valuable information on the volatility of HOM derived from α-pinene oxidation and also a methodology for the determination of volatility of organic species, especially for thermally labile species. I recommend the publication of this manuscript in ACP after the authors address several important issues as detailed below.

Major comments:

1.1 Referee comment 1

P16, Sect. 3.5. As shown in Fig. 6, the possible reactive or solubility-driven uptake of oxidation products resulted in a difference in the condensation behavior of some of HOM (both CHO compounds and organonitrates) between experiments with efflo-resced and deliquesced seeds. How big was this difference? To what extent this difference affected the determination of the fraction remaining of gas-phase HOM upon seed addition and hence their volatilities? A quantitative evaluation of the effect of particle-phase processes of HOM should be included in the revised manuscript.

1.1.1 Author response

The referee correctly identifies one of the limitations of the study, that is, the possibility of uptake of HOM driven by heterogeneous or particle phase processes, and not by volatility.

1. As for the more quantitative assessment of the difference between the effloresced and deliquesced cases, we have added a new subplot to Figure 6, showing a scatter plot of the fractions remaining between these two conditions. This should aid in assessing the magnitude of the difference and was something that referee 2 also requested.

2. As for the effect this has on the determination of the fraction remaining, and thus the assessment of the volatility of HOM: from the difference between the effloresced and deliquesced conditions, we know that there is an enhanced uptake of HOM in the deliquesced case, presumably caused by particle phase processes. Even the calculation of the condensation sink is more complicated in the humid case: however, we expect this effect to be minor (see response to reviewer 2, comment 2). However, we do not know the extent, if any, that particle phase processes play in the effloresced case. Therefore, the difference between the two conditions does not directly tell us anything about the potential particle phase processes in the effloresced case, just that there are some in the deliquesced case. Because of this, we use the effloresced, non-acidic seed conditions for the parametrization of the volatility. The possibility of particle phase processes affecting this condition as well is an inherent limitation of the study. By choosing the experiments with non-acidic, effloresced seed, we try to minimize the effect of this as best we can.

1.1.2 Changes to the manuscript

We have added a new subplot, detailing the difference between the effloresced and deliquesced cases (see response to comment 2 from reviewer 2). The possibility of particle phase processes affecting the results is acknowledged in the section ”2.4.4. Effect of heterogeneous chemistry on the gas phase”, including its last sentence (already present in the original manuscript): “Still, we cannot fully exclude the effect of particle phase processes on the response of HOM to seed addition.”, and in other parts of the manuscript.

1.2 Referee comment 2

In addition, since the HOM monomers and dimers may decompose after condensation, producing more volatile products that may partition back to the gas phase, I am curious if the authors observed any oxidation products showing an increase in their gas-phase concentrations upon seed addition.

1.2.1 Author response

We do indeed observe the increase of the concentrations of some compounds upon seed addition: these are visible with fractions remaining above one in Figures 5 and 6. This type of behaviour is only observed for a small number of compounds. However, we may not be sensitive to others that exhibit similar behaviour. We have added additional discussion on this in the manuscript. Also, we have excluded the compounds with FR over 1.1 from the statistical model.

1.2.2 Changes to the manuscript

We have added the following text when discussing the Figure 5:
"*Indeed, we observe some compounds with the values for fraction remaining above one, mainly at lower masses (Fig. 5): this implies an increased source term upon seed addition. Presumably these compounds are formed in the particle phase and are of high enough volatility to evaporate back to gas phase, as discussed in Sect. 2.4.4. However, the number of these compounds is small, and they lie mainly outside the HOM masses. So, while there are indications of some particle phase processes taking place, we expect that the volatility of a compound is dominant in determining their behaviour for the vast majority of the detected compounds.*"

1.3 Referee comment 3

P18, Sect. 3.6.1. In my understanding, the oxidation products that were possibly affected by the particle-phase processes represented a source of uncertainty in volatility determination and should be excluded from the model. However, these species were actually included in the model. The authors should explain this.

P21, L11. The authors stated that they couldn't exclude the role of particle-phase processes in artificially lowering HOM volatility estimated using their parameterization. Have the authors tried to develop a parameterization excluding HOM species affected by particle-phase processes from the model and compare the results with existing volatility estimates?

1.3.1 Author response

As noted in response to referee comment 1, we cannot readily distinguish those compounds that are affected by particle phase processes in the effloresced case. We only

know that there are indications that some compounds are affected in the deliquesced case. Excluding those compounds would not be justified, as we do not know the extent to which, if any, they are affected in the effloresced case. However, as noted in the reply to the previous comment, there were some compounds whose concentration increased during seed addition: this is a clear indication of particle phase processes affecting those compounds. We have now chosen to exclude any compounds with a fraction remaining above 1.1 (meaning a 10 % increase upon seed addition) from the statistical model, as these are clearly influenced by particle phase processes. However, there was only one such compound, so this plays no large role in determining the model fit.

1.3.2 Changes to the manuscript

We have excluded compounds with FR over 1.1 from the model, and added the following sentence in section 3.6.1: "*In addition, any compounds with a FR value over 1.1 (meaning a 10 % increase upon seed addition) were excluded due to the influence of particle phase processes on them.*"

We have also added the following sentences to section 3.6.1: "*Finally, the possibility that the uptake of some compounds to particles is not driven by their volatility, but rather some particle phase processes (as noted in Sect. 2.4.4) would affect the modelling as well. This would lead to artificially low volatility estimates. However, as noted above, we have tried to minimize this effect.*"

Minor comments:

1.4 Referee comment 4

P7, L16. I suggest the authors provide details as to how the wall loss lifetime of ELVOC was estimated from their condensation behavior upon seed addition.

1.4.1 Author response

ELVOC concentration is determined by their source strength and their lifetime in the gas phase, as noted in the manuscript. Assuming a constant source, any changes in the concentration are caused by changes in the lifetime. During a seed injection, the ELVOC concentration drops to a fraction of its original value: this drop is determined by the ratio of the gas phase lifetimes during and before seed injection. As the main determinants of the lifetime are the condensation sink and the wall loss, and we know the condensation sink, we can then use the known condensation sink and drop in ELVOC concentrations to estimate the wall loss. We validated this approach by comparing to the results of Ehn et al. (2014, 10.1038/nature13032), where the wall loss was directly measured. They used UV lights to produce high concentrations of OH radicals, which then reacted with a-pinene. This led to HOM formation, which could be instantaneously shut off by turning off the light. The wall loss lifetime was then calculated from the rapid decay of the gas phase HOM. There, the wall loss estimated from ELVOC drop during seed injection agrees strikingly well with the one estimated from UV switch off experiments. We have added details on the wall loss determination in the manuscript.

1.4.2 Changes to the manuscript

We reformatted the paragraph discussing the gas phase lifetime of ELVOC. The main changed text is: "*A typical condensation sink caused by particles formed in the chamber in the absence of inorganic seed was* 2×10^{-3} *s*$^{-1}$ *(Table A1), corresponding to*

a lifetime of 500 seconds with respect to the loss to particle surfaces. When adding seed particles, the typical condensation sink was 10×10^{-3} *s*$^{-1}$*. This corresponds to a lifetime of only 100 seconds with respect to the condensation to particle surfaces. Thus, the losses to condensation on aerosol particles are, to a first approximation, an order of magnitude faster than either the chemical sink or flush out. We do not have a direct measurement of the wall loss lifetime in the chamber. However, we can estimate it from the behaviour of ELVOC upon seed addition. Without any wall loss, the sink term of ELVOC would increase roughly fivefold, reflecting directly on the gas phase concentrations. However, the observed decrease in concentrations is smaller. A wall loss lifetime of 400 s explains the observed decrease in ELVOC well: this number is consistent across experiments. This was also a free parameter in the ADCHAM model, which yielded identical results.*"

1.5 Referee comment 5

P8, L12-14. Since the lifetime of gas-phase ELVOC depends on the condensation sink (CS). The authors should specify the value of CS leading to a 60

1.5.1 Author response

We have added the numbers.

1.5.2 Changes to the manuscript

The text now reads: "*Upon a typical seed injection experiment, the condensation sink increases from around* 2×10^{-3} *s*$^{-1}$ *to around* 10×10^{-3} *s*$^{-1}$*, and condensation onto aerosol particles becomes the main sink of ELVOC. This leads to the decrease of the gas phase lifetime of ELVOC by around 60 % (Fig. 1).*"

1.6 Referee comment 6

P12, L20. Replace “as well as” by “and”.

1.6.1 Author response

Replaced

1.7 Referee comment 7

P15, Fig. 5 and P17, Fig. 6. A logistic fit to the data in these figures may help to demonstrate the trend more obviously and also help to locate the transition mass between the high- and low-volatility limits.

1.7.1 Author response

This is something we considered when preparing the manuscript, but eventually decided against. This was for a couple of reasons. First, we present a logistic fit on the composition of the HOM later in the text. This is a better fit, as, like stated in the text, it is not really the mass of a compound that determines its volatility, but rather its chemical makeup. Presenting two logistic fits could be confusing to the reader, who might pick up on the relationship between the mass and the fraction remaining and thus volatility, instead of the more proper one between the molecular formula and the volatility. Also, for Fig. 6 a fit for the non-nitrates and organic nitrates separately would make more sense: this would be a hybrid between the fit on mass only, and the one on elemental composition. We feel it is better to stick to the fit on elemental composition. Further, as more of a subjective opinion, we feel that the trend is rather obvious already, and a fit would not add much value to the figure, while increasing the complexity unnecessarily.

Therefore, we decided to keep the figures without the fits.

1.8 Referee comment 8

P16, L6. Delete “in the differences”.

1.8.1 Author response

Deleted

1.9 Referee comment 9

P19, L4. Delete “the”.

1.9.1 Author response

Deleted

1.10 Referee comment 10

P24, Table A1. Why the numbering of experiments starts with 2? And the numbering of exps. 17-21 is not in numerical order.

1.10.1 Author response

This was a tentative numbering, used in the analysis phase. This included a failed, non-listed experiment 1, as well as the addition of experiment 21 later, when we realized

that there actually was good gas-phase data from that experiment as well, contrary to our initial impression. For clarity, we have changed the numbering to start from 1 and proceed in numerical order through the experiments, in chronological order.

1.10.2 Changes to the manuscript

We have changed the numbering, both in the table and in the text.

âĂČ

2 Anonymous Referee 2

Highly oxygenated organic molecules (HOM) play an important role in new particle formation, early growth and constitute a large fraction of secondary organic aerosol. To assess their role in these processes better, their volatilities should be known. However, their structures could so far not be identified and there are no easily accessible surrogate compounds. In this paper a method is presented to determine the volatility of HOMs. Ozonolysis of alpha-pinene was performed in a simulation chamber until a steady state concentration of HOMs was reached. After injection of a seed aerosol a new steady state concentration of HOMs was obtained. From the difference of the concentration of the two steady-states the volatility of HOMs could be derived. Using the chemical composition of the HOMs a relation between their volatility and their carbon, hydrogen, nitrogen and oxygen numbers was derived. It was found that volatility does decrease less with addition of an oxygen atom than predicted by other parameterizations reported in literature. Furthermore, the experiments were well simulated with the ADCHAM model. The results presented in this study are of high interest and well suited for ACP. The method used here is well suited and the experiments and data analysis were well done. The paper is also well written

and I recommend publication of this manuscript. There are a few points I would like the authors to clarify or add some more information and I also suggest some more additions to put the results presented here into the perspective of other works.

Major comments:

2.1 Referee comment 1

The main assumption for the analysis is that the source terms stay constant upon seed addition. The authors note that RO2 radicals decrease by less than 20 %. Now, the main reaction path to HOM for NOx-free conditions is by RO2+ RO2, since the RO2 concentration is much higher than HO2. Thus, the HOM formation rate could decrease considerably (40% max), if the total RO2 concentration would decrease by 20 %. Could you comment on this.

2.1.1 Author response

The 20 % decrease was an upper end estimate based on an RO2 lifetime of 10 seconds, with a high increase in CS during seed injection. This was meant more as an upper limit, but we now realize that it seems unnecessarily high. For a more typical increase of CS, the drop in RO2 lifetime would be less than 10 %. In addition, in the ADCHAM model the RO2 lifetimes are closer to 5 seconds, which would further decrease the drop.

Also, for most of the HOM monomers at least, the formation is probably through a reaction of a highly oxidized RO2 (HOM-RO2) with an early, much less oxidized RO2. What happens to these upon contact with seed particles is to our knowledge unknown. However, given that RO2 radicals in aqueous solution typically terminate through bi-

molecular reactions (https://doi.org/10.1016/S0273-1223(97)00003-6), we expect that the uptake of those RO2 to particles is not especially fast. If this is the case, and the less oxidized RO2 are not affected by seed addition, the drop in HOM source term for most compounds would come only from the drop in HOM-RO2 radicals. We performed some simulations using ADCHAM with enhanced uptake of the less oxidized RO2 to particles, but this deteriorated the fit between the model and the observations considerably. Thus, it seems that the less oxidized RO2 indeed are not much affected by the seed addition.

For the highly oxidized HOM dimers, which require two HOM-RO2 to form, the decrease in source term would be quadratic to the HOM-RO2 decrease, as noted. However, we observe no clear trend of increasing drop in concentrations with increasing oxygen content of the dimers. Therefore, we assume this effect to be minor, but still worth mentioning as a limitation in the manuscript. We also added an example from Garmash et al. (2019, acpd, 10.5194/acp-2019-582): in an analogous situation, they observe a larger than predicted drop of HOM upon seed addition: this is explained by multi-generation OH oxidation, where both the precursor and the HOM itself drop upon seed addition, resulting in a larger HOM loss from the gas phase.

2.1.2 Changes to the manuscript

We re-formatted the paragraph discussing RO2 loss to seed particles. We added the following sentences: "*Upon contact with seed particles or chamber walls, similarly to ELVOC, the highly oxidized RO_2 can be expected to be lost from the gas phase. However, this only becomes an important sink for them if their chemical lifetime is long enough to allow for non-negligible condensation. If this is the case, seed addition may influence their concentration.*"

And changed the sentence with the 20 % drop to: "*During a typical seed injection, the gas phase lifetime of RO_2, and thus their concentration, are expected to drop by less*

than 10 %"

And added the following subsection: "**A note on multi-generation oxidation** *We have so far considered oxidation products originating directly from VOC oxidation, through short-lived RO_2 intermediates. In the case of HOM from α-pinene, this is a good approximation (Bianchi et al., 2019). In contrast, in some systems, oxidation products may undergo repeated oxidation by e.g. hydroxyl radicals, leading to production of more oxidized products. This is observed in the case of aromatics Garmash et al. (2019). In this case, both the HOM formed in the repeated oxidation, and the precursor, itself an oxidation product, may condense on seed particles. Garmash et al. (2019) observed some compounds dropping more than expected upon seed addition, and explained this in terms of multi-generation oxidation. This is a clear example where the decrease of a gas phase compound upon seed addition does not only depend on its volatility, but the volatility of its precursors as well. However, in the case of α-pinene the vast majority of HOM form directly from the oxidation of α-pinene, and thus this effect should be minor (Bianchi et al., 2019).*"

2.2 Referee comment 2

Page 16, line 33ff: Do you see difference for both types of seeds at 40% RH compared to 1% RH? It is difficult to see the differences from Figure 6. Would it be better visible using a scatter plot between the two RH systems? The condensation sink is calculated from the dry seed diameter. At 40% RH the particles are larger. How much would this influence the fraction remaining?

2.2.1 Author response

Yes, the difference is similar in AS dry vs. wet and in ABS dry vs. wet. Further, there is no big difference between AS wet and ABS wet, like there is no big difference between

AS and ABS dry.

We agree that judging the differences between experiments by eye is challenging and subjective: as suggested, we have added scatter plots to aid in the comparisons of experiments. We added two scatter plots: the first details the (non)difference between the non-nitrate monomers in the no-NOx and NOx experiments (so between the first and the second sigmoid plot), as Figure 6b. The second details the difference between the dry vs. humid cases (the two sigmoid plots in the figure 6): this is the new figure 6d.

It is true that the condensation sink is calculated for the dry particles, and this is an underestimation in the humid case. The exact values of the condensation affect the fraction remaining for nonvolatile species, with higher condensation sink giving lower fraction remaining. With increasing CS, the position of the "lower arm" of the sigmoid curve will shift downwards: however, the general behavior should not be affected. Also, in the further analyses for explaining the fraction remaining, we used only the dry experiments. Therefore, we feel that trying to account for the effect of RH on the condensation sink would bring unnecessary complexity to the analyses, without contributing to the results or their interpretation.

2.2.2 Changes to the manuscript

We have added two new subplots to the Figure 6: the new figure, along with its updated caption, is also shown at the end of the document.

In addition, we have added a few lines comparing the findings for the AS vs ABS seed to our earlier study: "*However, in the same set of experiments, Riva et al. (2019) found a large SOA enhancement on dry ABS seed particles. The lack of difference in the gas-phase HOM concentrations indicates that the increase in SOA did not come from enhanced HOM uptake, as measured by the* NO_3^- *-CI-APi-TOF. Indeed, Riva et*

al. (2019) observe a marked decrease of more volatile gas-phase oxidation products, including pinonaldehyde, upon ABS seed addition."

2.3 Referee comment 3

Figure 7: The observed values seem to be systematically lower than the modeled ones at lower fraction remaining. It looks like there is still a sigmoidal dependence. How was the weighting of the signals done? Does it strongly influence the fit?

2.3.1 Author response

The fitting of the model was done using the Matlab function fitglm, and the weighting of the observations using the option "Weight". In essence, this fits a generalized linear model, giving more weight to the compounds with a high signal in the estimation. This is good for two reasons: their values for fraction remaining are less uncertain, and in this way the model better describes the majority of the HOM observed. We further investigated the behaviour of the fitted vs. observed values for fraction remaining and have updated Fig. 7. Most of the compounds for which the observed values were lower than the modelled ones have a carbon number lower than 10. In contrast, most C10 compounds are fitted well, and probably play a large role in determining the model fit. This can indicate that the dependence of the fraction remaining (FR) on the oxygen number is not the same for all carbon numbers (e.g. that the FR for C8 compounds would drop more steeply upon oxygen addition than it does for C10 compounds). This could, to some extent, be described in the model by including an appropriate interaction term. However, this would complicate the model quite a bit. We feel that the current, simple model describes the data well enough not to justify a more complex model. We have added discussion on this in the manuscript. We have also changed the signal-to-noise criterion to be stricter for the compounds to be included in the model.

2.3.2 Changes to the manuscript

We have updated figure 7: the updated version is shown below. The sentence "*Larger deviances from the 1:1 line are mainly explained by carbon numbers lower than ten.*" was added to the caption.

We have also added the following discussion in section 3.6.1: "*Out of the monomers, the abundant C_{10} compounds are fitted the best, appearing close to the 1:1 line. The compounds deviating from this line mainly have a smaller carbon number: C_9 compounds seem especially problematic for the model. This could be an indication that the dependence of the volatility on e.g. the oxygen number is different for compounds with fewer than 10 carbon atoms. Both organic nitrates and non-nitrates seem to be fitted equally well.*"

2.4 Referee comment 4

Page 20, line 1ff: I suggest to also show in this discussion an example for a known compound of higher volatility, e.g. pinic acid, pinonic acid. I have the feeling that this relationship only holds for compounds with multiple peroxy groups.

2.4.1 Author response

We agree that this relationship is probably specific for autoxidation products. Older parametrizations, specifically fitted for compounds of higher volatility, may work better for non-autoxidation systems. We have now added an explicit mention of this in the manuscript. Also, we have added the examples of pinic and pinonic acid in the discussion.

2.4.2 Changes to the manuscript

We have added the following sentences to the section in question: "*Also, the relationship presented in Eq. (11) may not hold for oxidation systems other than the one presented here, or indeed compounds formed in α-pinene oxidation, but not through autoxidation. Examples of products formed in the latter way include pinic ($C_9H_{14}O_4$) and pinonic acids ($C_{10}H_{16}O_3$). Equation (11) gives them saturation concentrations 15 μg m^{-3} and 27 μg m^{-3}, respectively, compared to literature values in the range of a couple of μg m^{-3} for pinic and from less than one to up to hundreds of μg m^{-3} for pinonic acid (Bilde and Pandis, 2001; Salo et al., 2010; Donahue et al., 2012). Especially for pinonic acid the spread in literature values is very large. Given that HOM are chemically quite different from the two acids, the agreement is surprisingly good. Still, any generalizations should be drawn with caution.*"

2.5 Referee comment 5

Table 1: It is difficult to grasp all the information in the table. I suggest to present it also in a figure O:C versus log C*, as it is often done in literature. This could make the dependencies better visible. Furthermore, could you also compare your volatilities with other measurements, e.g. from FIGAERO (D'Ambro et al., Earth Space Chemistry 2018, 2, 1058-1067; Schobesberger et al., ACP 18, 14757-14785, 2018). Although these measurements are from the particle phase they still cover similar types of compounds.

2.5.1 Author response

We agree that the table was difficult to grasp and have replaced it with a figure containing the same information.

As noted, in Schobesberger et al. and D'Ambro at al. the volatility measurements are from the particle phase. The method is based on thermal desorption, and in all cases presented the authors needed thermal decomposition of oligomers, in addition to the evaporation of free monomers, to explain the thermograms. Thus, the thermo/evapograms were always explained as a combination of at least two volatilities. In addition, while the compounds they investigate are similar to HOM, they mainly have less oxygen. Due to these reasons, we have decided not to include comparison to those measurements.

2.5.2 Changes to the manuscript

We have replaced the table with a plot, see the end of the document. The caption remains almost the same.

2.6 Referee comment 6

Page 22 line 11; Figure A2: The authors suggest to use their new parameterization in future studies. In the simulation of Figure A2, their model uses the SIMPOL parameterization. I wonder, how their new parameterization would affect the simulation? Does it give similar results?

2.6.1 Author response

We realize that the wording for the suggestion was too strong, and have reworded.

We tested to use our parametrization for the volatilities of HOM in the ADCHAM model, but this did not change the results significantly. In the ADCHAM model, we used a nucleation parametrization from Kirkby et al. (2016, 10.1038/nature17953), that assumes

all non-nitrate HOMs to nucleate. Hence, the parametrized nucleation rate does not depend on the volatilities of HOM. Further, in the presence of seed, most HOM will condense anyway. Therefore, further investigations are required to assess the effect of the exact volatility parametrization on particle formation.

2.6.2 Changes to the manuscript

The sentence suggesting to use our parametrization now reads: "*Future studies should evaluate the effect of the exact volatility parametrization used on new particle formation from HOM.*"

Minor comments:

2.7 Referee comment 7

Page 1, line 18: Replace hyrdoxy by hydroxyl. This also occurs several times later in the text.

2.7.1 Author response

Corrected the typos

2.8 Referee comment 8

Page 4, line 20: Did you also correct for hygroscopic growth as in Dal Maso et al.?

2.8.1 Author response

No, we used the dry condensation sink directly. See also response to referee 2, comment 2. Dal Maso et al. have a parametrization to typical Hyytiälä hygroscopic growth, which would most probably be wrong in our case. Also, as noted in the previous reply, the exact values of the condensation sink are not too important for the conclusions.

2.8.2 Changes to the manuscript

We have added the following sentences to the part in question: "*We did not correct for hygroscopic growth of the particles, so in humid cases the calculated condensation sink is an underestimate: however, this should not have any notable effect on the conclusions.*"

2.9 Referee comment 9

Page 12, line 10; Here you say that you excluded compounds with SD-to-signal ratio higher than 4. How can you evaluate a signal at such high noise? In Figure 5 it says compounds with a signal to noise ratio above 4 have been excluded and on page 18, line 13 it states compounds with a signal to noise ratio below 4 have been excluded. I assume only the last statement is correct.

2.9.1 Author response

Yes, the wording was all messed up, and only the last statement was correct. Now we have corrected these, and in addition changed the S/N criterion for the binomial model to be more strict (exclude compounds below ten).

2.10 Referee comment 10

Figure 2: Color of shading is different from what is stated in the Figure caption.

2.10.1 Author response

Caption fixed

2.11 Referee comment 11

Figure 3: You report here experiment seven. How can you model this without knowledge of CS during SS1?

2.11.1 Author response

The experiment was mislabeled by accident: in reality, this was experiment nine (where the CS is known). And with the new numbering scheme of the experiments (see referee 1, comment 10), it becomes experiment eight.

2.11.2 Changes to the manuscript

Corrected the numbering

2.12 Referee comment 12

Figure 5: Is the scaling linear?

2.12.1 Author response

Yes, surface area scales linearly with signal. We have now added an explicit mention of this in the captions of figures 5 - 7.

Interactive comment on Atmos. Chem. Phys. Discuss., https://doi.org/10.5194/acp-2019-620, 2019.

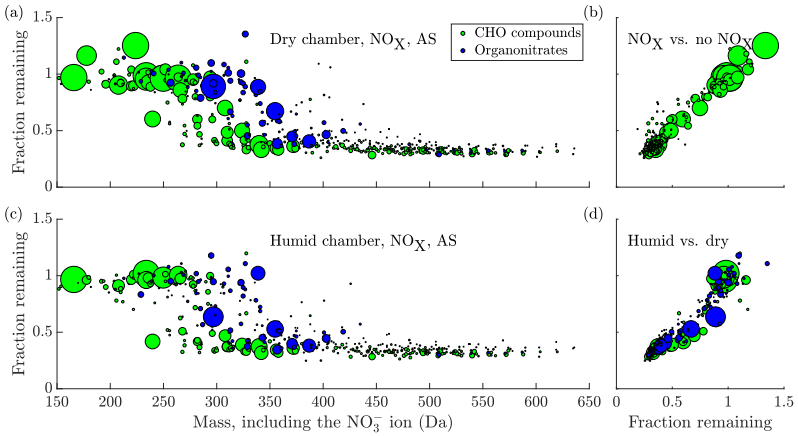

Fig. 1.

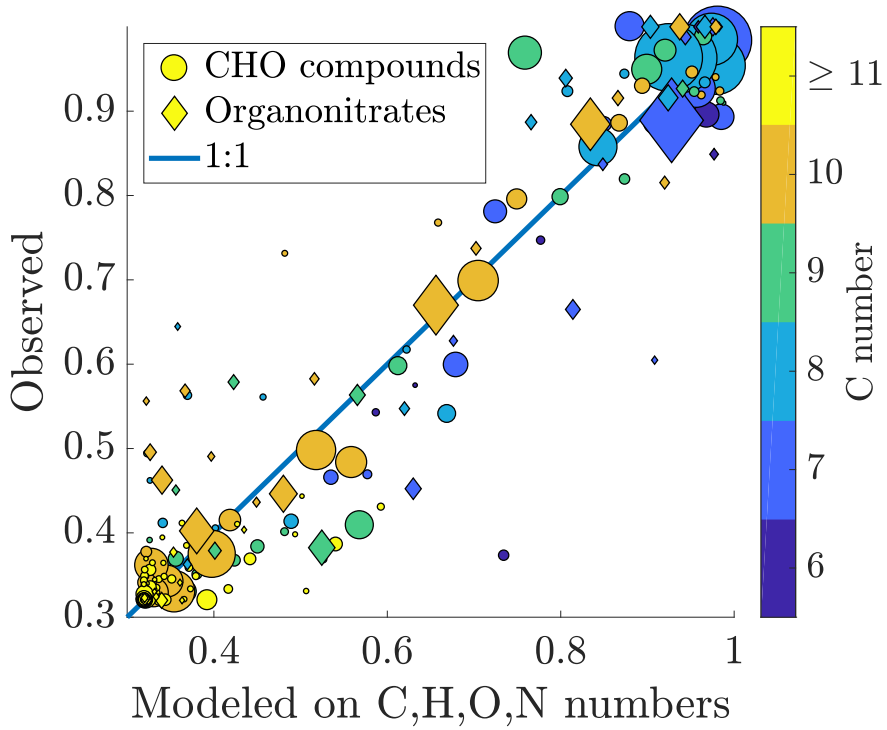
CHO compounds
Organonitrates
1:1
Observed
Modeled on C,H,O,N numbers
C number
≥ 11
10
9
8
7
6
0.3
0.4
0.5
0.6
0.7
0.8
0.9
0.4
0.6
0.8
1

Fig. 2.

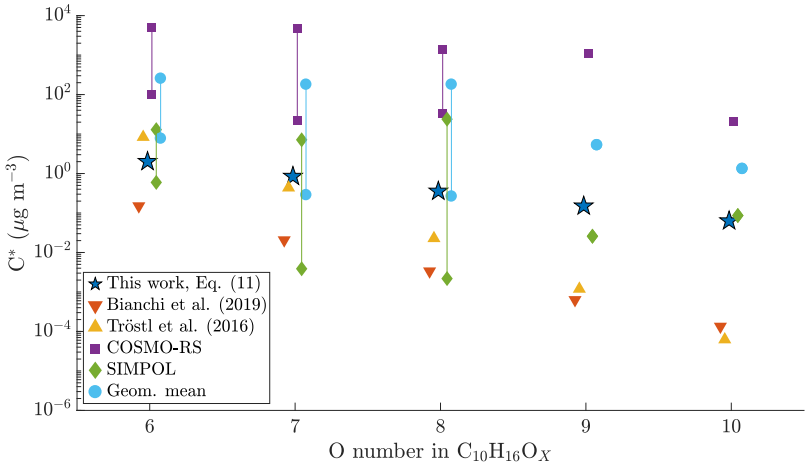
This work, Eq. (11)
Bianchi et al. (2019)
Tröstl et al. (2016)
COSMO-RS
SIMPOL
Geom. mean
C* (μg m⁻³)
O number in C10H16OX
10^4
10^2
10^0
10^-2
10^-4
10^-6
6
7
8
9
10

Fig. 3.

Experimental investigation into the volatilities of highly oxygenated organic molecules (HOM)

Otso Peräkylä[1], Matthieu Riva[1, 2], Liine Heikkinen[1], Lauriane Quéléver[1], Pontus Roldin[3], and Mikael Ehn[1]

[1]Institute for Atmospheric and Earth System Research / Physics, Faculty of Science, University of Helsinki, Finland
[2]Univ Lyon, Université Claude Bernard Lyon 1, CNRS, IRCELYON, F-69626, Villeurbanne, France
[3]Division of Nuclear Physics, Lund University, P.O. Box 118, 22100 Lund, Sweden

Correspondence: Otso Peräkylä (otso.perakyla@helsinki.fi) and Mikael Ehn (mikael.ehn@helsinki.fi)

Abstract. Secondary organic aerosol (SOA) forms a major part of the tropospheric submicron aerosol. Still, the exact formation mechanisms of SOA have remained elusive. Recently, a newly discovered group of oxidation products of volatile organic compounds (VOC), highly oxygenated organic molecules (HOM), have been proposed to be responsible for a large fraction of SOA formation. To assess the potential of HOM to form SOA, and to even take part in new particle formation, knowledge of their exact volatilities would be essential. However, due to their exotic, and partially unknown, structures, estimating their volatility is challenging. In this study, we performed a set of continuous flow chamber experiments, supported by box modelling, to study the volatilities of HOM, along with some less oxygenated compounds, formed in the ozonolysis of α-pinene, an abundant VOC emitted by the boreal forests. Along with gaseous precursors, we periodically injected inorganic seed aerosol into the chamber to vary the condensation sink (CS) of low volatility vapours. We monitored the decrease of oxidation products in the gas phase in response to increasing CS, and were able to relate the responses to the volatilities of the compounds. We found that HOM monomers are mainly of low volatility, with a small fraction being semi-volatile. HOM dimers were all of at least low volatility, but probably of extremely low volatility: however, our method is not directly able to distinguish between the two. We were able to explain the volatility of the oxidation products in terms of their carbon, hydrogen, oxygen and nitrogen numbers. We found that increasing levels of oxygenation correspond to lower volatilities, as expected, but that the decrease is less steep than would be expected based on many existing models for volatility, such as SIMPOL. The hydrogen number of a compound also explained its volatility, independently of the carbon number, with higher hydrogen numbers corresponding to lower volatilities. This can be explained in terms of the functional groups making up a molecule: high hydrogen numbers are associated with e.g. ~~hyrdoxy~~ hydroxy groups, which lower the volatility more than e.g. carbonyls, that are associated with a lower hydrogen number. The method presented should be applicable to systems other than α-pinene ozonolysis, and with different organic loadings in order to study different volatility ranges.

1 Introduction

Secondary organic aerosol (SOA) makes up a major fraction of the tropospheric submicron aerosol world-wide (Zhang et al., 2007; Jimenez et al., 2009). Despite its importance and much research effort, our fundamental understanding of the formation

of SOA has remained lacking (Hallquist et al., 2009; Shrivastava et al., 2017). Recently, a new group of oxidation products of volatile organic compounds (VOCs), highly oxygenated organic molecules (HOM, Ehn et al., 2014, 2017; Bianchi et al., 2019), has been proposed to be the source of a major fraction of tropospheric submicron SOA (Ehn et al., 2014). Important sources of HOM include many monoterpenes, the most abundant group of biogenic VOCs emitted by boreal forests.

Most VOCs form organic peroxy (RO_2) radicals upon oxidation. HOM form through the autoxidation of these organic peroxy radicals, a process only recently discovered to be important in atmospheric oxidation (Crounse et al., 2013; Ehn et al., 2014). An extensive description of HOM formation can be found in Bianchi et al. (2019). Briefly, in autoxidation, RO_2 radicals undergo intramolecular hydrogen abstractions, followed by the addition of molecular oxygen on the resulting carbon-centered radical. This results in a new RO_2 radical, with an additional hydroperoxy group. This process can repeat multiple times. The radical reaction chain can be terminated unimolecularly, through the loss of an OH radical from the RO_2 radical, resulting in a closed shell oxidation product. It can also be terminated bimolecularly, for example through the reaction with another RO_2 radical, or nitric oxide (NO). The termination mechanism is important in determining which types of HOM form in the reaction. As an example, the bimolecular termination with another RO_2 radical can very efficiently lead to the formation of molecular dimers of extremely low volatility (Berndt et al., 2018b, a), and the termination with NO can lead to the formation of organic nitrates. Due to the fast autoxidation process, combined with the different termination mechanisms, the products can rapidly acquire high oxygen contents, with those having at least six oxygen atoms counted as HOM (Bianchi et al., 2019). The oxygen appears in the form of many functional groups, including carbonyl, hydroperoxy, hydroxy, peroxy acid and carboxylic acid groups (e.g. Mentel et al., 2015).

Due to the high level of functionalization, HOM are thought to be of low volatility (Bianchi et al., 2019). This is supported by observations that HOM are efficient in forming SOA, and even able to take part in the very first steps of new particle formation (NPF) (Ehn et al., 2014; Kirkby et al., 2016). To determine exactly to what extent HOM can impact NPF and SOA formation, the knowledge of their vapour pressures is essential (Bianchi et al., 2019). Still, determining the vapour pressures of HOM remains challenging. Most of the species have not been isolated, hampering experimental characterization (Bianchi et al., 2019). Due to the high numbers of functional groups, estimating the vapour pressures with commonly used functional group contribution methods is not sufficient, and different computational approaches give estimates of the vapour pressures spanning many orders of magnitude (Kurtén et al., 2016). In order to investigate the volatility of HOM formed in the ozonolysis of α-pinene, Ehn et al. (2014) used injections of inorganic seed aerosol to increase the condensation sink in a chamber experiment. They observed the behaviour of HOM to be consistent with kinetically limited condensation and extremely low volatilities, but only looked at the sum of HOM, not focusing on individual compounds. Thus, and also based on existing composition-volatility relationships, HOM were initially classified as extremely low volatility organic compounds (ELVOC, according to the definitions by Donahue et al., 2012). Theoretical work by Kurtén et al. (2016) has later suggested that the most HOM, especially the monomers, might not be ELVOC, but low volatility organic compounds or even semi-volatile organic compounds (LVOC and SVOC respectively, again according to Donahue et al., 2012). Thus, detailed information on HOM volatility is still lacking, which presents a key obstacle for assessing their impact on particle formation (Bianchi et al., 2019).

Here, we investigate the volatility of HOM, along with some less oxygenated compounds, experimentally, in a manner similar to Ehn et al. (2014), but on a molecular level. We produce HOM in the ozonolysis of α-pinene in a continuous flow smog chamber, and measure them in the gas phase with the nitrate Chemical Ionization Atmospheric Pressure interface Time of Flight mass spectrometer (CI-APi-TOF, Jokinen et al., 2012). We inject inorganic seed aerosol into the chamber, and monitor how the gas phase concentrations of the oxidation products change. We show that we can gain valuable and detailed information about the volatility of the oxidation products using this method. Further, we develop a parametrization describing the volatility of HOM formed in the ozonolysis of α-pinene, especially the monomers, in terms of their composition, and compare the results to existing parametrizations and estimates on HOM volatility.

2 Methods

2.1 Chamber set-up

In order to investigate the volatility of HOM formed in the gas phase in a controlled manner, we conducted a series of laboratory experiments in the newly constructed COALA chamber at the University of Helsinki, previously presented by Riva et al. (2019). The chamber is a two cubic metre bag, made of teflon (FEP) foil with dimensions (L × W × H) 1650 × 1100 × 1100 mm and 0.125 mm thickness, supplied by Vector Foiltec (Bremen, Germany). The chamber is contained in a rigid enclosure with 400 nm LED lights to photolyse nitrogen dioxide (NO_2) to NO, and is stirred with a teflon fan to ensure homogeneous mixing of the air inside. The chamber was operated in a continuous flow mode, with a residence time of 50 minutes, attained by setting the inflow to the chamber to 40 litres per minute (Lpm). In the continuous flow mode the total flow out of the chamber was the same as the inflow. The instrumentation (Sect. 2.2) sampled the majority of the flow out of the chamber. The chamber was maintained at a slight overpressure, resulting in the rest of the flow being flushed to an exhaust line.

We injected dry air purified with a clean air generator (AADCO model 737-14, Ohio, USA) into the chamber, along with gaseous reactants α-pinene, O_3, and in some of the experiments, NO_2. Ozone was generated by injecting purified air through an ozone generator (Dasibi 1008-PC), while α-pinene and NO_2 were from gas bottles. The injections were controlled with a range of mass flow controllers (MKS, G-Series, 0.05-50 Lpm, Andover, MA, USA). We controlled the relative humidity in the chamber to be either < 1 % or 40 %: this was done by bubbling the dry clean air through a bubbler filled with purified (Milli-Q) water.

In addition to the gaseous reactants, we injected size selected, 80 nm inorganic seed particles, consisting of either ammonium sulfate (AS) or ammonium bisulfate (ABS), into the chamber. ABS was used in order to promote acidity-dependent particle phase reactions: the effect of these on the particle phase has been presented by Riva et al. (2019). The particles were produced by atomizing a solution consisting of Milli-Q water and AS or Milli-Q water and ABS, after which the seed particles were dried for size selection. After size selection, the particles were either injected into the chamber as dry, or subjected to a relative humidity of over 80 % to attain deliquescence before injection into the chamber. In the < 1 % RH experiments, we only used the dried particles, while in the 40 % RH experiments, both types were used.

2.2 Instrumentation

We monitored the chamber with a suite of online instruments measuring both gas and particle phases. For measuring the responses of HOM and other oxidation products of α-pinene to the seed injections, we used the nitrate CI-APi-TOF (TOFWERK AG, Aerodyne, Jokinen et al., 2012), equipped with a long time-of-flight (LTOF) mass analyzer for a resolving power of over 13 000 in the HOM mass range (300 – 650 Da). The instrument can detect highly oxygenated compounds as clusters with the nitrate ion (NO_3^-). It allows for the determination of the molecular formulae of the detected clusters due to its high mass resolution. Along with closed shell products, the CI-APi-TOF can detect certain highly oxidized RO_2 radicals as well. As the method is based on the soft clustering of the analyte molecules with the nitrate anion, we assume that any multiple charging effects are negligible. Thus, the charge that the detected ions carry is always assumed to be -*e*, and the measured mass-to-charge ratios to directly correspond to masses. We express the masses in daltons (Da).

We used a Proton Transfer Reaction Time-Of-Flight mass spectrometer (PTR-TOF 8000, Ionicon, Graus et al., 2010) to measure the concentration of the reactant α-pinene, and a UV photometric ozone monitor (Model 49p, Thermo Environmental Instruments) for the ozone concentration. For measuring the NO_X concentration we used a chemiluminescence NO-NO_2-NO_X analyzer (Model 42i, Thermo Fisher Scientific), and for the NO concentration the more sensitive Ecophysics CLD 780 TR.

For the particle phase measurements, we used a differential mobility particle sizer (DMPS, Aalto et al., 2001) and a high resolution aerosol mass spectrometer (HR-AMS, DeCarlo et al., 2006), also equipped with the LTOF analyzer. We used the DMPS for the determination of the dry aerosol size distribution in the chamber between 10 and 400 nm, and the AMS for the chemical composition of the dried particles.

From the DMPS size distribution, we also calculated the dry condensation sink (CS), describing the ability of a particle size distribution to remove low-volatility vapours from the gas phase (Dal Maso et al., 2005). CS depends on the molecular diffusion coefficient and mean molecular speed of a compound: thus, the value of CS is compound-dependent. Instead of the often used values for sulfuric acid, we calculated the condensation sink specifically for HOM. The molecular diffusion coefficient was calculated using Fuller's method (Tang et al., 2015), and the mean molecular speed was calculated using kinetic theory. Both the molecular diffusion coefficient and speed depend on molecular composition and on the absolute temperature during the experiments. The values presented for the condensation sink are calculated for the compound $C_{10}H_{16}O_7$, and are around 40 % lower than for sulfuric acid. In comparison, the CS calculated for the largest molecules (i.e. HOM dimers) were approximately 30 % lower than for $C_{10}H_{16}O_7$. We did not correct for hygroscopic growth of the particles, so in humid cases the calculated condensation sink is an underestimate: however, this should not have any notable effect on the conclusions.

2.3 Overview of experiments

In a typical experiment, we first continuously injected only gaseous precursors α-pinene, O_3, and in some of the experiments, NO_2, into the dry or humidified chamber. In the experiments with NO_2, we also used 400 nm LED lights to photolyse NO_2 to NO. We used two intensities for the LED lights: these corresponded to steady state NO concentrations of around 100 and 200 ppt with around 30 ppb of NO_2. During the injection of gaseous precursors, we observed particle formation. The injection was

continued until a steady state had been reached with respect to both the gas phase and the particle phase. After sampling the steady state chamber for a number of hours, we started injecting either AS or ABS particles, either dried or deliquesced. The injection was continued until a new steady state had been reached, and been sampled for a number of hours. The duration of a typical experiment was eight hours without the inorganic seed, and eight hours of seed injection. The temperature during the experiments was around 302 K. An overview of experimental condition is presented in Table A1.

2.4 Continuous flow chamber dynamics

The time evolution of the gas phase concentration of a compound in the chamber is determined by its sinks (S) and sources (Q). The sources of a compound to the gas phase consist of its injection into the chamber, its chemical production in the gas phase in the chamber, and its evaporation from chamber walls and aerosol particles. Its sinks, on the other hand, consist of its flush out from the chamber, its loss to chemical reactions, and its condensation onto walls and aerosol particles. In an actively mixed chamber, such as the one used, the concentration of compounds is homogeneous across the chamber. Thus, the effect of sources and sinks on the concentration of a compound X in the chamber can be expressed as follows:

$$\frac{\mathrm{d[X]}}{\mathrm{dt}} = Q_{\text{injection}} + Q_{\text{chemical}} + Q_{\text{wall}} + Q_{\text{aerosol}} - S_{\text{flush out}} - S_{\text{chemical}} - S_{\text{walls}} - S_{\text{aerosol}}. \quad (1)$$

In a continuous flow chamber, given that the inflow of reactants is kept constant, a steady state is eventually reached. In a steady state, the sources and sinks of a compound are equal, and thus its time derivative in Eq. (1) goes to zero and its concentration stays constant. The time required for the formation of a steady state varies between components in the chamber. In the following section we present some limiting cases of gas phase compounds and the steady states formed between their sources and sinks.

2.4.1 Effect of volatility on the behaviour of compounds in the gas phase

The volatility of a gas phase compound affects the type of steady state it forms in the chamber. Next we will qualitatively outline which terms in Eq. (1) are important for different types of compounds, and how those affect the types of steady states, as well as the sensitivities of those steady states to seed injections to the chamber.

For volatile reactants like α-pinene (AP in equations), the loss by condensation to either chamber walls or aerosol particles is negligible. In other words, condensation will be followed by prompt evaporation back to the gas phase. In this case, the condensation and evaporation terms in Eq. (1) can be omitted. Furthermore, α-pinene is not chemically produced in the gas phase, but injected into the chamber. Thus, the injection is the only source term remaining, while the loss terms are the chemical loss and flush out of the chamber. In a steady state, we can write the Eq. (1) for α-pinene as follows:

$$Q_{\text{AP, injection}} = S_{\text{AP, flush out}} + S_{\text{AP, chemical}}. \quad (2)$$

Injection rate of α-pinene is kept constant, independently of the concentration in the chamber. In contrast, the rate at which α-pinene is flushed out of the chamber is directly proportional to its concentration in the air leaving the chamber, which is the same as the concentration in the chamber. The chemical sink is caused by the oxidation of α-pinene, and is dependent on the concentrations of both α-pinene and its oxidants. In this study, we injected ozone into the chamber to oxidize α-pinene. In the ozonolysis reactions of alkenes, hydroxyl (OH) radical is also produced: for α-pinene, the yield is close to one (Atkinson et al., 1992; Paulson and Orlando, 1996). OH goes on to react with α-pinene. Further, in the experiments with NO_2 injected, some nitrate (NO_3) radical is produced, which also reacts with α-pinene. We can thus expand Eq. (2):

$$\begin{aligned} Q_{\text{AP, injection}} &= S_{\text{AP, flush out}} + S_{\text{AP, chemical}} \\ &= (k_{\text{flush out}} + k_{\text{O}_3+\text{AP}}[\text{O}_3]_{\text{SS}} + k_{\text{OH+AP}}[\text{OH}]_{\text{SS}} + k_{\text{NO}_3+\text{AP}}[\text{NO}_3]_{\text{SS}})[\text{AP}]_{\text{SS}} \\ [\text{AP}]_{\text{SS}} &= \frac{Q_{\text{AP, injection}}}{k_{\text{flush out}} + k_{\text{O}_3+\text{AP}}[\text{O}_3]_{\text{SS}} + k_{\text{OH+AP}}[\text{OH}]_{\text{SS}} + k_{\text{NO}_3+\text{AP}}[\text{NO}_3]_{\text{SS}}}, \end{aligned} \tag{3}$$

where SS refers to steady state conditions, and $k_{\text{flush out}}$ is the reciprocal of the chamber turnover time, 50 minutes. Q_{AP} represents the injection rate of α-pinene into the chamber, which is kept constant throughout an experiment. Thus, the steady state α-pinene concentration is determined by its input to the chamber, the steady state concentrations of the oxidants, and the turnover time.

Similarly to α-pinene, oxidation products of relatively high volatility, such as intermediate volatility organic compounds (IVOC, Donahue et al., 2012), do not readily condense on aerosol particles with loadings used in our experiment (Table A1). However, it is possible that some of the compounds partition onto the chamber walls. This is due to the observation that, with respect to the partitioning of organic vapours, Teflon walls of smog chambers behave in a manner similar to a very high organic aerosol loading (e.g. Matsunaga and Ziemann, 2010; Krechmer et al., 2016). The extent of the partitioning of the compounds to the walls varies depending on e.g. their volatility. Thus, the evaporation and condensation terms related to aerosol particles in Eq. (1) can be assumed negligible, but the corresponding terms for wall interactions not.

The oxidation products of α-pinene generally have lost their carbon-carbon double bond upon the initial oxidation reaction. This means that they are unreactive towards ozone, but can still be oxidized by the OH and NO_3 radicals formed in the chamber. Thus, the sinks of gas phase IVOC in the chamber include their potentially reversible loss to chamber walls, flush out of the chamber, and chemical sink to reactions with radicals. As the oxidation products are not directly injected into the chamber, but produced in the oxidation of α-pinene, the sources include their chemical production and evaporation from walls. Therefore, we can express their steady state concentration as follows:

$$\begin{aligned} Q_{\text{IVOC, chemical}} + Q_{\text{IVOC, wall}} &= S_{\text{IVOC, flush out}} + S_{\text{IVOC, chemical}} + S_{\text{IVOC, walls}} \\ &= (k_{\text{flush out}} + k_{\text{OH+IVOC}}[\text{OH}]_{\text{SS}} + k_{\text{NO}_3+\text{IVOC}}[\text{NO}_3]_{\text{SS}} + k_{\text{IVOC, walls}})[\text{IVOC}]_{\text{SS}} \\ [\text{IVOC}]_{\text{SS}} &= \frac{Q_{\text{IVOC, chemical}} + Q_{\text{IVOC, wall}}}{k_{\text{flush out}} + k_{\text{OH+IVOC}}[\text{OH}]_{\text{SS}} + k_{\text{NO}_3+\text{IVOC}}[\text{NO}_3]_{\text{SS}} + k_{\text{IVOC, walls}}}, \end{aligned} \tag{4}$$

where the $k_{\text{IVOC, walls}}$ is the wall loss rate coefficient for IVOC, and evaporation from walls is expressed in terms of the wall source. Here the sink of the IVOC is thus independent of the condensational aerosol surface area in the chamber. This means that the volatility of the compound is high enough that there is no net condensation in the time scale of the chamber turnover. It is important to note that the wall source for IVOC is not necessarily constant, but may depend on temperature, humidity and chamber history through the accumulation of IVOC on the chamber walls.

Like IVOC, oxidation products of low volatility, such as ELVOC, are not directly injected into the chamber, but produced from α-pinene oxidation in the gas phase. Because of their extremely low volatility, their evaporation into the gas phase from either aerosol particles or chamber walls is negligible. Instead, they are lost by irreversible condensation to the particles and walls. In addition, they are flushed out of the chamber, and lost by oxidation reactions with radicals. In a steady state, the sources and sinks are equal and we can write

$$\begin{aligned} Q_{\text{ELVOC, chemical}} &= S_{\text{ELVOC, flush out}} + S_{\text{ELVOC, chemical}} + S_{\text{ELVOC, walls}} + S_{\text{ELVOC, aerosol}} \\ &= (k_{\text{flush out}} + k_{\text{OH+ELVOC}}[\text{OH}]_{\text{SS}} + k_{\text{NO}_3\text{+ELVOC}}[\text{NO}_3]_{\text{SS}} + k_{\text{ELVOC, walls}} + \text{CS}_{\text{ELVOC}})[\text{ELVOC}]_{\text{SS}} \\ [\text{ELVOC}]_{\text{SS}} &= \frac{Q_{\text{ELVOC, chemical}}}{k_{\text{flush out}} + k_{\text{OH+ELVOC}}[\text{OH}]_{\text{SS}} + k_{\text{NO}_3\text{+ELVOC}}[\text{NO}_3]_{\text{SS}} + k_{\text{ELVOC, walls}} + \text{CS}_{\text{ELVOC}}}, \end{aligned} \tag{5}$$

where CS_{ELVOC} is the condensation sink for ELVOC, caused by aerosol particles, and $k_{\text{ELVOC, walls}}$ is the wall loss rate. The sinks together determine the average lifetime of an ELVOC molecule in the gas phase, and Eq. (5) can also be written in terms of the lifetime, τ_{ELVOC}:

$$[\text{ELVOC}]_{\text{SS}} = Q_{\text{ELVOC, chemical}}\tau_{\text{ELVOC}}. \tag{6}$$

We ~~estimate, from their behaviour upon seed addition, that the wall loss lifetime of ELVOC is on the order of 400 seconds in the COALA chamber. The flush out lifetime is the same as the chamber residence time, 50 minutes, or 3000 seconds. We~~ do not know the exact reaction rate coefficients between ELVOC species and OH, or the OH concentration in the chamber. To get an upper limit for the chemical loss, we can assume a collision limited reaction similarly to Bianchi et al. (2019), and production of OH from every ozone-α-pinene reaction, with α-pinene acting as the main OH sink. With these assumptions, we estimate the lifetime of ELVOC towards OH radical reactions to be on the order of 2000 seconds. Using similar reasoning, the contribution of reactions with the nitrate radical should be at maximum comparable to the OH reactions, but probably much smaller. ~~This means that without any aerosol in the chamber, the majority of ELVOC are lost to condensation onto chamber walls (Fig. 1).~~ A typical condensation sink caused by particles formed in the chamber in the absence of inorganic seed was 2×10^{-3} s^{-1} (Table A1), corresponding to a lifetime of 500 seconds with respect to the loss to particle surfaces. ~~In this case, the largest fraction of ELVOC would still be lost to the chamber walls (Fig. 1). In contrast, when~~ When adding seed particles, the typical condensation sink was 10×10^{-3} s^{-1}. This corresponds to a lifetime of only 100 seconds with respect to the condensation to particle surfaces. ~~This means that by~~ Thus, the losses to condensation on aerosol particles are, to a first approximation, an order of magnitude faster than either the chemical sink or flush out. We do not have a direct measurement of

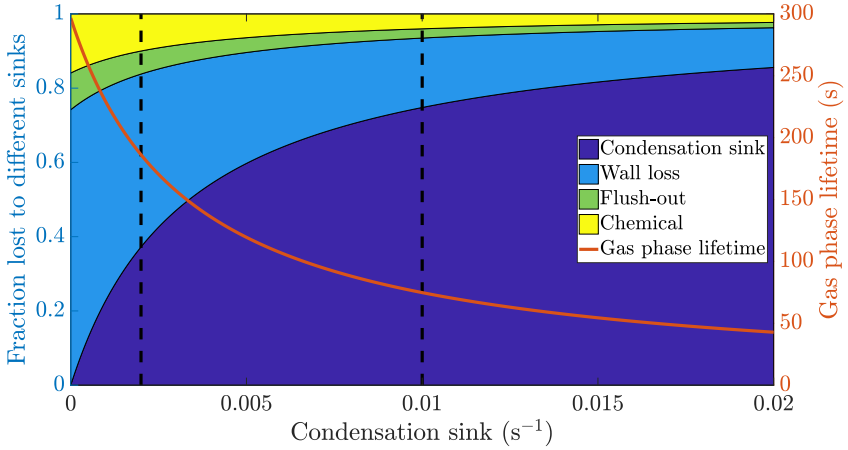

Figure 1. The calculated fraction of ELVOC lost to different sinks, and their total lifetime in the gas phase as a function of the condensation sink caused by aerosol particles in the chamber. The wall loss lifetime of ELVOC is ~~assumed~~ estimated to be 400 seconds . The chemical loss is an upper limit estimate, based on an OH concentration of around 0.1 ppt and collision limited reaction with ELVOC. The vertical broken lines at 0.002 s^{-1} and 0.01 s^{-1} represent a typical situation without seed particles and with seed particles, respectively (Table A1).

the wall loss lifetime in the chamber. However, we can estimate it from the behaviour of ELVOC upon seed addition. Without any wall loss, the sink term of ELVOC would increase roughly fivefold, reflecting directly on the gas phase concentrations. However, the observed decrease in concentrations is smaller. A wall loss lifetime of 400 s explains the observed decrease in ELVOC well: this number is consistent across experiments. This was also a free parameter in the ADCHAM model, which yielded identical results. This means that that without seed addition, the majority of ELVOC are lost to condensation onto chamber walls (Fig. 1). By introducing inorganic seed aerosol, we can change the dominating loss term of ELVOC from their condensation to the chamber walls to their condensation to aerosol surfaces, and at the same time decrease their lifetime in the gas phase by around 60 % (Fig. 1). Assuming that the source term remains unchanged, the decreased steady state lifetimes are directly reflected in the gas phase concentrations of the ELVOC (Eq. (6)). This drop of around 60 % corresponds to a case when there is only negligible evaporation of the oxidation products back from the particle phase in the time scale of the chamber lifetime. In addition to ELVOC, this may include low volatility organic compounds (LVOC) from the lower end of their volatility spectrum. Thus, their net loss by condensation is limited by their molecular diffusion to the particle and wall surfaces, not equilibrium partitioning. If the source term of a given compound is unchanged, this represents an upper limit for how much the seed addition can drop the gas phase signal. The exact magnitude of this drop varies from experiment to experiment, since there is some variability in the condensation sink both with and without seed aerosol (Table A1).

Based on the example cases of IVOC and ELVOC, we can outline how seed injections affect oxidation products of different volatilities. In the case of IVOC, the volatility of the product is high enough that there is negligible net condensation. Thus, the sink of the compound is unchanged upon seed addition. Assuming that the source of the compound stays constant, the

seed injection has no effect on the gas phase concentration of the compound. For ELVOC, the gas-to-particle conversion is irreversible. Upon ~~seed injection~~a typical seed injection experiment, the condensation ~~into~~ sink increases from around 2×10^{-3} s^{-1} to around 10×10^{-3} s^{-1}, and condensation onto aerosol particles becomes the main sink of ELVOC~~, and the~~. This leads to the decrease of the gas phase lifetime of ELVOC ~~decreases~~ by around 60 % (Fig. 1). If the ELVOC source remains constant, this decrease of the lifetime results in a 60 % drop in the gas phase concentration of ELVOC. For compounds with volatilities between these extremes, such as semi-volatile organic compounds (SVOC), the gas phase concentration can be affected, but not as much as for ELVOC. In order to assess the exact effect of the volatility of an oxidation product on its behaviour upon seed injection, we performed model simulations with the ADCHAM model, explained in more detail in Sect. 2.5.

Above, we have assumed that the source term of oxidation products stays constant upon seed injection. In the following section, we will present two important cases when this assumption does not hold, and discuss their effect on the method and the results. The first case is related to the loss of RO_2 radicals, important intermediates in the α-pinene oxidation, to seed surfaces. The second case is related to the production of compounds on the chamber walls or in aerosol particles, and their subsequent evaporation to the gas phase.

2.4.2 Dynamics of organic peroxy radicals in the chamber

An important class of intermediates in the formation of HOM from the ozonolysis of α-pinene are organic peroxy radicals (RO_2). These compounds are reactive, both towards other RO_2 and radicals such as NO and HO_2, as well as through unimolecular decomposition (e.g. Ehn et al., 2014; Jokinen et al., 2014). ~~If~~ Upon contact with seed particles or chamber walls, similarly to ELVOC, the highly oxidized RO_2 can be expected to be lost from the gas phase. However, this only becomes an important sink for them if their chemical lifetime is long enough ~~that their loss to particle surfaces becomes a~~ to allow for non-negligible ~~sink for them, they can be affected by the seed addition~~condensation. If this is the case, seed addition may influence their concentration. This is an important consideration for our study. With the injections of inorganic seed aerosol, we wish to alter the sink of non-volatile oxidation products, without affecting their source. Under the conditions in our chamber, and using the reaction rate coefficients used by Ehn et al. (2014) to describe HOM formation, a lifetime of the RO_2 radicals of around 10 seconds can be expected. With such a chemical lifetime, the condensation of RO_2 on aerosol particle surfaces becomes a non-negligible, but minor, sink. During a typical seed injection, the gas phase lifetime of RO_2, and thus their concentration, are expected to drop by ~~no more than 20~~ less than 10 % (Fig. A1). This would in turn decrease the source term for all closed shell oxidation products formed in the reactions of the RO_2 radical. However, compared to the 60 % reduction in the gas phase lifetime of the oxidation products upon seed addition (Fig. 1), the reduction in the source rate would be a minor effect. Still, it is important to keep in mind that any changes observed in the concentrations of gas phase oxidation products during seed injections can be caused by changes to their sources, their sink, or a combination of both.

2.4.3 A note on multi-generation oxidation

We have so far considered oxidation products originating directly from VOC oxidation, through short-lived RO_2 intermediates. In the case of HOM from α-pinene, this is a good approximation (Bianchi et al., 2019). In contrast, in some systems, oxidation

products may undergo repeated oxidation by e.g. hydroxyl radicals, leading to production of more oxidized products. This is observed in the case of aromatics (Garmash et al., 2019). In this case, both the HOM formed in the repeated oxidation, and the precursor, itself an oxidation product, may condense on seed particles. Garmash et al. (2019) observed some compounds dropping more than expected upon seed addition, and explained this in terms of multi-generation oxidation. This is a clear example where the decrease of a gas phase compound upon seed addition does not only depend on its volatility, but the volatility of its precursors as well. However, in the case of α-pinene the vast majority of HOM form directly from the oxidation of α-pinene, and thus this effect should be minor (Bianchi et al., 2019).

2.4.4 Effect of heterogeneous chemistry on the gas phase

So far we have only explicitly considered the formation of compounds in the gas phase oxidation. However, particle phase processes can potentially affect the gas-phase concentrations of compounds as well. A compound X, after condensation, can be chemically transformed in the particle phase. If the resulting product, Y, is sufficiently volatile, it can evaporate back to the gas phase:

$$\mathrm{X(g)} \rightarrow \mathrm{X(p)} \rightarrow \mathrm{Y(p)} \rightarrow \mathrm{Y(g)}. \tag{7}$$

This process can affect the gas phase concentrations in two ways. First, the concentration of compound Y can increase during a seed injection due to the process. Secondly, in addition to the effect of volatility, there is a chemical sink for compound X in the particle phase. This results in less evaporation back to the gas phase than would be expected based on volatility alone, and a larger decrease in gas phase concentration. This would in turn be interpreted as a lower than actual volatility. We cannot readily distinguish between chemical reaction driven uptake and physical condensation due to low saturation vapour pressures. However, in the experiments with crystalline ammonium sulfate particles, we assume particle phase reactions to be very slow. In contrast, the use of ammonium bisulfate and deliquesced seed particles were in part motivated by particle phase reaction enhancement (e.g. Riva et al., 2019). Thus, by comparing the different experiment types, we can gain insight into the different uptake mechanisms. Still, we cannot fully exclude the effect of particle phase processes on the response of HOM to seed addition.

2.5 Modelling the behaviour of HOM in the chamber upon seed injection

In order to quantitatively relate the volatilities of the formed oxidation products to the behaviour of their gas phase concentrations under the seed injection, we performed a series of simulations using the ADCHAM model (Roldin et al., 2014). The gas phase chemistry in ADCHAM was simulated using the Master Chemical Mechanism v3.3.1 α-pinene chemistry (Jenkin et al., 1997; Saunders et al., 2003) and the recently developed Peroxy Radical Autoxidation Mechanism (PRAM) (Roldin et al., 2019). In short, we used the measured temperature, relative humidity, concentration of ozone and α-pinene and chamber flow rates as input to the model. The inorganic seed aerosol was represented by a particle number size distribution similar to the one used in the experiments. Further, the modelled AS or ABS particle mass concentration was kept identical to the one measured

with the AMS. This was achieved by, for every model time step, adding new seed particles to the chamber in an amount equal to the concentration difference between the modelled dry seed particle mass, from the previous time step, and the measured mass, from the present time step. The modelled steady state particle number size distribution, without seed particles, was evaluated against the DMPS observations and optimized by tuning the new particle formation rate of particles with an initial diameter of 1.5 nm. The SOA formation in the model was represented by treating all organic vapours with a saturation concentration (C^*) < 10^3 μg m^{-3} as potentially condensable. The pure-liquid saturation vapour pressures (p_0) of the organic vapours were calculated using the SIMPOL functional group contribution method (Pankow and Asher, 2008). In addition to the condensable vapour from the gas-phase mechanism, we also introduced 15 oxidation products of predetermined C^* in the range 10^4 to 10^{-3} μg m^{-3}, all having a fixed Q_{chemical} equal to 10^{-5} molec cm^{-3} s^{-1}. By tracking the behaviour of the relative concentration drop of these model compounds, before and after the seed injections, we could connect this to representative C^*, for conditions similar to the actual chamber experiment.

The reversible wall losses of the condensable vapours were modelled using the method proposed by Matsunaga and Ziemann (2010). In this method, the vapour loss rate to the chamber walls and the evaporation of the same vapours from the walls back to the gas-phase are represented by two different first order rate coefficients k_{wall} and $k_{\text{wall,back}}$. For each individual condensable organic compound (i), k_{wall} was estimated using Eq. (8) and $k_{\text{wall,back}}$ with Eq. (9):

$$k_{\text{wall},\,i} = \frac{1}{400}\sqrt{\frac{D_i}{D_{\text{C}_{10}\text{H}_{16}\text{O}_7}}}, \tag{8}$$

$$k_{\text{wall, back},\,i} = k_{\text{wall},\,i}\frac{p_{0,i}}{C_{\text{wall}}RT}. \tag{9}$$

The Teflon walls are treated as a large organic aerosol concentration (C_{wall}), which absorb the organic vapour molecules that hit the walls. We used a C_{wall} equal to 100 μmol m^{-3}, which is within the range of values reported by Matsunaga and Ziemann (2010). D_i and $D_{\text{C}_{10}\text{H}_{16}\text{O}_7}$ in Eq. (8) are the molecular diffusion coefficients for compound *i* and the reference HOM molecule $C_{10}H_{16}O_7$, respectively. R is the ideal gas constant (8.3145 J K^{-1} mol^{-1}) and T is the temperature in Kelvin. The organic compound molecular diffusion coefficients were calculated with Fuller's method (Tang et al., 2015). Equation (8) takes into account that large organic molecules have a slower diffusion than small molecules and therefore lower k_{wall}. As an example, for a HOM dimer with molecular formula $C_{20}H_{30}O_{16}$ the first order wall loss rate becomes 1/481 s^{-1} (17 % lower than for $C_{10}H_{16}O_7$).

2.6 Interpretation of the CI-APi-TOF data

The vast majority of the ions detected with the CI-APi-TOF were clusters of analyte molecules with the nitrate ion, NO_3^-. However, a minor fraction appeared to be analyte molecules clustered with the dimer of nitric acid, $(HNO_3)NO_3^-$, as seen before by e.g. Bianchi et al. (2016, supplementary information). Analyte molecules that do not contain nitrogen, clustered with the dimer of nitric acid, appear at exactly the same masses as some organic nitrates clustered with only the nitrate ion. However, they are seen even without nitrogen oxides (NO_X) in the chamber, when no organic nitrates are formed. Further proof of their

identity as non-nitrates clustered with the nitric acid dimer comes from the good correlation of their time behaviour with that of the corresponding peaks clustered only with the nitrate ion. Due to this, for the analyses during the experiments without NO_X in the chamber, we excluded any peaks containing more than one nitrogen atom, i.e. the one from the nitrate ion. In the presence of NO_X, we observed a large increase in the signals at these masses, attributed to the formation of organic nitrates appearing at the same masses. In these experiments, the organic nitrates probably contributed the clear majority to these signals, but there was a non-zero contribution from the dimer charging as well. This should be taken into account when interpreting the results. In general, we observed that the dimer clustering seemed to be more prominent with the LTOF instrument used here, compared to the older high resolution APi-TOFs (HTOFs).

In addition to the analyte molecules charged with the nitrate ion or its dimer, some molecules are also detected as deprotonated anions. For simplicity, we excluded these peaks from the analyses.

RO_2 radicals formed in the ozonolysis or OH oxidation of α-pinene, and organic nitrates containing one nitrate group, both have an odd number of hydrogen atoms, causing them to appear at odd masses in the spectra. Further, the difference in mass is often very small. This causes problems for the separation of the signals originating from RO_2 radicals from those coming from organic nitrates (or non-nitrate compounds charged with the dimer of nitric acid, as noted above). The signals may not be unambiguously separated, and the signal attributed to one may have some contribution from the other. For this reason, we do not present detailed results on the behaviour of RO_2 radicals during seed injection. Organic nitrates often have much higher signals as compared to RO_2 radicals, which makes their fits more robust (Cubison and Jimenez, 2015). Due to this, we do present results on their behaviour. However, due to the overlap with some RO_2 radicals, along with the dimer charging effect discussed above, these results should be interpreted with some caution.

2.7 Data processing

We processed the nitrate CI-APi-TOF data using tofTools (Junninen et al., 2010). After high resolution peak fitting, we normalized the signal intensities by the sum of the reagent ion signals, taking into account the nitrate monomer, dimer and trimer signals. We then used these normalized signals in subsequent analysis. As the analysis focuses on relative changes in signal intensities, absolute concentration calibrations were not necessary.

In order to investigate the effect of seed injections on gas phase concentrations of α-pinene oxidation products, we compared the signal levels during the seed injections to those during the steady state before the injection. For assessing the reliability of the signals, we calculated the mean signal level during the steady state before the seed injection, along with the standard deviation (SD) of the signal during this period. A high standard deviation in relation to the mean signal level can mean either a noisy signal, or an unstable one. For this reason, we excluded the compounds with a SD-to-mean ratio ~~above~~ below four from further analyses.

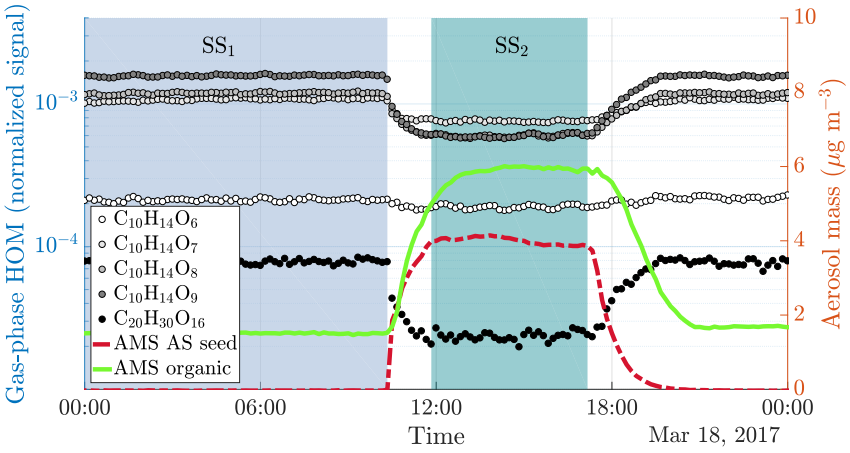

Figure 2. Time series of both gas and particle phase species during a typical seed injection (Experiment 19, Table A1). The experiment starts with only gaseous precursors being injected into the chamber: these form HOM (dotted lines, measured with the NO_3^--CI-APi-TOF), which form SOA (solid green line, measured with the AMS). Both the HOM and the SOA are in a steady state (SS_1, ~~green~~ blue shading). At around 10 o'clock, we start injecting ammonium sulfate seed aerosol (red dashed line). This results in an increased condensation sink, which causes an increase in the SOA mass, and a decrease in the gas phase HOM signals. After a transition period, a new steady state is reached (SS_2, ~~red~~ turquoise shading). Upon stopping the seed injection, the SOA levels decrease again, and the HOM signals increase.

3 Results

3.1 General behaviour of HOM and organic aerosol upon seed injections

When injecting only gaseous precursors we observed formation of both HOM monomers and dimers, as expected. The HOM formation was accompanied by the formation of SOA. During the course of an experiment, both the HOM signals measured by the CI-APi-TOF, and the organic mass measured by the AMS, stayed stable, indicating they were in steady state (SS_1 in Fig. 2). After sampling this steady state for several hours, we started injecting inorganic seed aerosol. The seed aerosol concentration reached a steady level after a few hours (SS_2 in Fig. 2). This increase in the seed aerosol concentration resulted in an increased condensation sink, leading to enhanced condensation of HOM, and a corresponding increase in the organic aerosol mass (Fig. 2). The behaviour of both gas-phase HOM ~~, as well as the SOA ,~~ and SOA were well captured with the ADCHAM model (Fig. A2).

3.2 Expected relationship between vapour pressure and condensation behaviour of HOM

Using the ADCHAM model, we found that in the conditions of the chamber, the gas phase concentrations of oxidation products with a saturation concentration (C^*) over 100 μg m^{-3} (in the volatile end of the SVOC range) are not expected to be affected by the seed additions due to fast evaporation. Thus, the experimental setup cannot readily give precise information on the

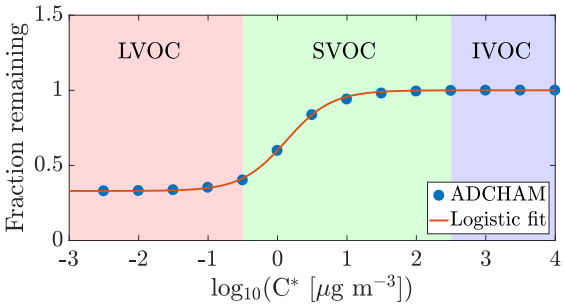

Figure 3. Modelled fraction remaining vs. the logarithm of saturation concentration from the ADCHAM model for experiment number ~~seven~~ eight (Table A1). In addition to the discrete data points representing model compounds in ADCHAM (Sect. 2.5), a logistic fit to them, with the formula ~~$y = \frac{1-0.33}{1+e^{-3.0(x-0.13)}}$~~ $y = \frac{1-0.33}{1+e^{-3.0(x-0.13)}} + 0.33$, is shown. Shading according to the volatility classes by Donahue et al. (2012).

volatilities of compounds having saturation concentrations above this value. At the other extreme, products with saturation concentrations below 0.01 μg m^{-3} (within the LVOC range) are expected to all show a behaviour consistent with irreversible condensation. Between these limiting cases, there is a smooth transition across the SVOC and upper end of LVOC range: it is in this area that the method can give the most precise information on volatility. (Fig. 3).

The response of the HOM to the seed injection was not uniform: some compounds showed a larger fractional decrease than others. As an example, only a small fraction of the original concentration of $C_{10}H_{14}O_9$ remained in the gas phase, while the concentration of $C_{10}H_{14}O_6$ was almost unaffected (Fig. 2). To better assess the exact magnitude of the decrease, we normalized the gas phase signal of each identified compound in the CI-APi-TOF spectrum to its level during the steady state before the seed injection (Fig. 4). In the experiment shown, the gas phase concentration of $C_{10}H_{14}O_6$ decreased only by around 10 % (Fig. 4). This decrease can be explained by a saturation concentration of around 5 μg m^{-3}, which lies well within the SVOC range. In contrast, the concentration of the more highly oxygenated $C_{10}H_{14}O_9$ decreased by more than 60 %, indicating a saturation concentration of around 0.2 μg m^{-3}, on the volatile end of LVOC range. The analogous compounds with seven and eight oxygen atoms exhibited behaviours between the two, showing a progression towards larger decreases with increasing oxygen number. This progression can be expected if we expect that the volatility of HOM gradually decreases with increasing level of oxygenation. In comparison to the monomers, the decrease in the gas phase concentration of $C_{20}H_{30}O_{16}$, an example of an essentially non-volatile HOM dimer, was slightly greater in magnitude to the decrease of $C_{10}H_{14}O_9$. This decrease of around 70 % is consistent with kinetically limited condensation, and behaviour expected of essentially non-volatile vapours. It also demonstrates the loss of sensitivity to large changes in volatility below around 0.3 μg m^{-3}: the saturation concentration of $C_{20}H_{30}O_{16}$ is presumably orders of magnitude smaller than that of $C_{10}H_{14}O_9$, yet they differ only slightly in their condensation behaviour.

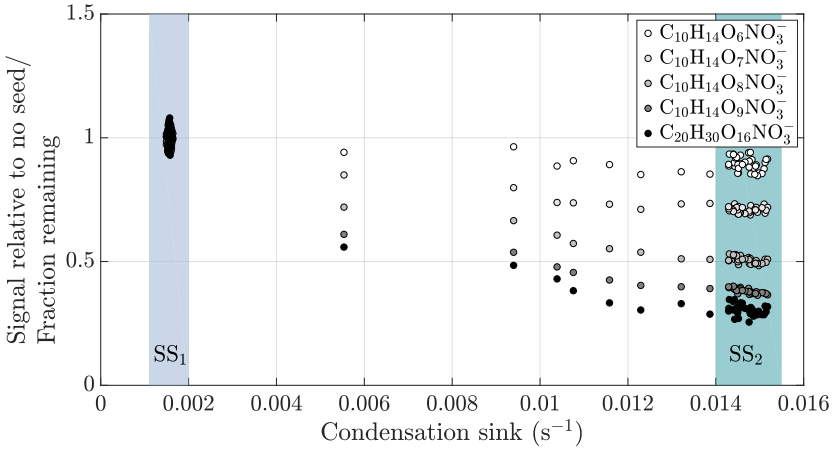

Figure 4. Gas phase HOM signal normalized to level before seed injection vs. condensation sink during a typical experiment (Experiment 19, same as in Fig. 2). The steady state before seed injection (SS_1) is visible as a cluster of points having a low condensation sink, and normalized gas phase signals of around 1. The steady state formed during the seed injection (SS_2) is seen as distinct clusters of points at higher condensation sink: the transition between the steady states is visible between these clusters. For each compound separately, we averaged the values during the seed injection steady state, and used these average values in the subsequent analyses.

3.3 Condensation behaviour of HOM as a function of molecular mass and composition

We will next analyze the behaviour of the measured gas phase compounds in experiments conducted in a dry chamber, without NO_X, using ammonium sulfate seed particles. We will then compare these results to those measured in the presence of NO_X, in a humid chamber, and using ammonium bisulfate instead of ammonium sulfate. To facilitate the analysis, we averaged the values for the fraction remaining for each fitted compound during the seed injection steady state, as demonstrated in Fig. 4, for each experiment separately. We then used these steady state average values for the fraction remaining in subsequent analyses.

Looking at the fraction remaining after seed injection as a function of the mass of the detected cluster, we generally observed values close to one for many of the lower mass compounds, up to 250 Da (including 62 Da from the charging nitrate ion) (Fig. 5). This indicates that the volatilities of these compounds generally fall into the volatile end of the SVOC, or IVOC range, or higher (Fig. 3). At the other end of the spectrum, we observed values around 0.3, indicating volatilities in the LVOC range or lower, for most high mass compounds starting from 350 Da (Fig. 5). Between the masses 250 Da and 350 Da there was a gradual, but consistent shift from the values close to 1 to values close to 0.3. This transition had a distinct sigmoidal shape, much like the transition of the expected fraction remaining with decreasing volatility, based on the ADCHAM model (Fig. 3). At the masses below 250 Da, we detect molecular fragments with a carbon skeleton shorter than that of the precursor α-pinene, and relatively few oxygen atoms. Due to their short carbon skeletons and low level of oxygenation, they are expected to be relatively volatile. On the other hand, on masses above 350 Da, we mainly detect the most oxidized HOM monomers with more than 10 oxygen atoms, along with HOM dimers. These compounds are expected to have low, or even extremely low,

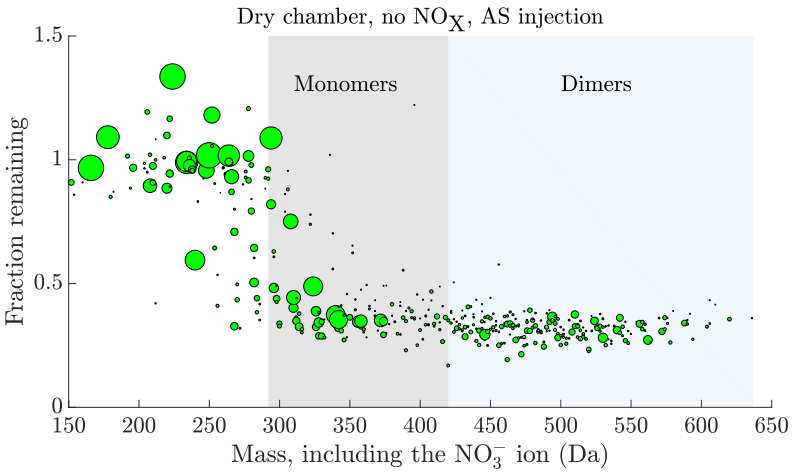

Figure 5. ~~Molecular~~ Fraction remaining after seed injection vs. the molecular mass of the detected cluster~~vs. the fraction remaining after seed injection.~~ The area of the circles has been linearly scaled to the magnitude of the signal of each compound before the seed injection, capped at 3.2×10^{-3}. The data are the average of experiments ~~2~~ 1 and ~~12~~11, with ammonium sulfate injection, dry chamber, and no NO_X in the chamber. Compounds with a signal to noise ratio, as defined in Sect. 2.7, ~~above~~ below 4 have been excluded from the plot. Characteristic HOM monomer and dimer regions have been highlighted with grey and blue shading, respectively.

volatility (Ehn et al., 2014; Kurtén et al., 2016; Tröstl et al., 2016; Bianchi et al., 2019). Between these extremes the sigmoid-like transition of compounds is consistent with a gradual decrease of volatility with increasing mass, coinciding with increased levels of oxygenation of the compounds. This transition seems to be centered around 310 Da: around this mass, the highest signals seem to be around half way between the high- and low volatility limits, i.e. with a saturation vapour concentration of around 1 μg m^{-3} (Fig. 3). The behaviour of the compounds during the seed injection thus seems consistent with what we would expect based on the presumed volatilities of the oxidation products. However, as stated in Sect. 2.4, we cannot exclude the possible role of a changed source term, or reactive uptake, for some of the compounds in determining the change in their gas phase concentrations during the seed injection. ~~Still, we~~ Indeed, we observe some compounds with the values for fraction remaining above one, mainly at lower masses (Fig. 5): this implies an increased source term upon seed addition. Presumably these compounds are formed in the particle phase and are of high enough volatility to evaporate back to gas phase, as discussed in Sect. 2.4.4. However, the number of these compounds is small, and they lie mainly outside the HOM masses. So, while there are indications of some particle phase processes taking place, we expect that the volatility of ~~the compounds~~ a compound is dominant in determining their behaviour for the vast majority of the detected compounds.

In addition to the closed shell products, we also investigated the effect of the seed additions on the highly oxidized RO_2 radicals measured with the CI-APi-TOF. However, due to the limitations listed in Sect. 2.6, we will not go into detail regarding the the behaviour of RO_2. Nonetheless, we observed some decrease in the signals attributed to them during the seed injections, but these decreases generally did not exceed 20 % of their signal before the seed addition. This further supports the idea that the majority of the changes observed in the closed shell species upon seed addition are indeed caused by differences in their

volatility, and not in ~~the differences in~~ their source terms. It seemed that the decrease in the concentrations of individual RO_2 was not entirely uniform, potentially indicating differences in their lifetimes and/or formation dynamics. We are investigating this phenomenon, and its effect on the formation of closed shell HOM, in more detail, and will publish these results separately.

3.4 Effect of NO_X

Upon introduction of NO_X in the chamber, we observed the formation of many oxidation products containing nitrogen (Fig. 6 (a)). These compounds are expected to form when RO_2 radicals are terminated by NO (Ehn et al., 2014), or when the oxidation is initiated by the nitrate radical (Yan et al., 2016): both result in the oxidation products containing an organic nitrate functional group. Compared to the experiments without NO_X, the behaviour of the non-nitrate oxidation products did not seem to change significantly (~~Figs. 5 and 6 (a~~Fig. 6 (b)). In contrast, compared to the oxidation products consisting of only carbon, hydrogen, and oxygen, the organic nitrates seemed to transition to low volatilities at markedly higher masses, with the transition centered around 355 Da (Fig. 6 (a), again including 62 Da from the charging nitrate). This is around 45 Da higher than for the non-nitrates. This difference in mass for compounds of similar volatility is to be expected based on the functional groups making up these oxidation products. Non-nitrate HOMs are expected to contain carbonyl, hydroperoxide, hydroxide, peroxyacid and carboxylic acid groups, in agreement with known reaction pathways for peroxy radicals (Ehn et al., 2014). The organic nitrate HOMs contain the nitrate group as well, acquired in the radical termination reaction with NO (or the initiation of the oxidation with NO_3). In the absence of NO, many termination pathways of RO_2 radicals lead to the formation of a hydroxy group (Vereecken and Francisco, 2012). While the nitrate group has a mass of 62, the ~~hyrdoxyl~~ hydroxy has a mass of only 17 Da. Despite their mass difference, they are expected to lower the volatility of a compound by roughly the same amount (Kroll and Seinfeld, 2008; Pankow and Asher, 2008). Hence, for two otherwise identical compounds, one containing a hydroxy group and the other a nitrate group, a similar volatility can be expected, while the organic nitrate has a mass 45 Da higher. This is analogous with a situation where a peroxy radical gets terminated either through reaction with NO or with HO_2, as an example: the resulting oxidation products show a large difference in mass, but have similar volatilities. Of course, these are not the only possibilities for the formation of organic nitrates and non-nitrates, but highlight that the mass difference for compounds of similar volatility is to be expected.

3.5 Effect of seed composition and chamber humidity on the condensation behaviour of HOM

Compared to the injections of ammonium sulfate, we did not find a large difference in the behaviour of the gas phase oxidation products ~~measured with the NO_3^--CI-APi-TOF~~ upon injections of the more acidic ammonium bisulfate. However, in the same set of experiments, Riva et al. (2019) found a large SOA enhancement on dry ABS seed particles. The lack of difference in the gas-phase HOM concentrations indicates that the increase in SOA did not come from enhanced HOM uptake, as measured by the NO_3^--CI-APi-TOF. Indeed, Riva et al. (2019) observe a marked decrease of more volatile gas-phase oxidation products, including pinonaldehyde, upon ABS seed addition.

In contrast, we did observe a difference between the experiments conducted at < 1 % RH with effloresced seed, and those at 40 % RH with deliquesced seed, with many compounds seeming to decrease more during seed addition in the humid chamber

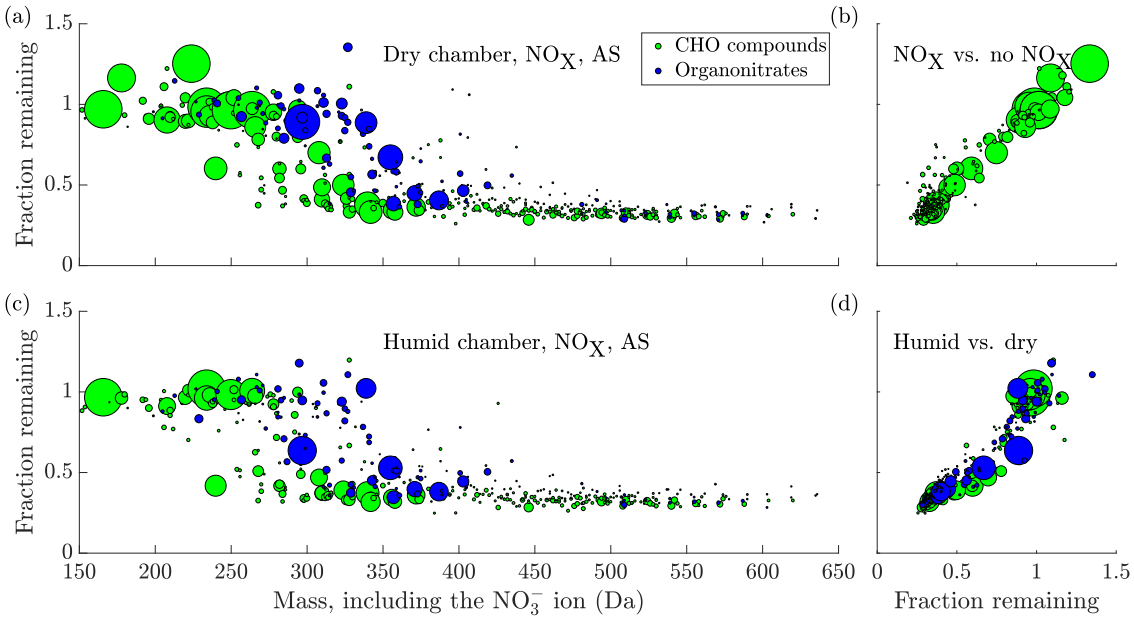

Figure 6. (a) ~~Molecular~~ Fraction remaining after seed injection vs. the molecular mass of the detected cluster, including the charging NO_3^- ion~~, vs. the fraction remaining after seed injection.~~ Area of the circles scaled linearly to the magnitude of the signal of each compound before the seed injection, capped at 3.2×10^{-3}. The data are the average of the experiments ~~16~~ 15 and 19, with ammonium sulfate injection to dry chamber, in the presence of NO_X. Compounds with a signal-to-noise ratio, as defined in Sect. 2.7, ~~above~~ below 4 have been excluded from the plot. **(b)** Comparison of the experiment in (a) to the no-NO_X case in Fig. 5. The y-axis and circle size are the same as in (a), with the fraction remaining from Fig. 5 on the x-axis. Only CHO compounds are plotted, as organonitrates are not formed in the experiments without NO_X. There is a general linear agreement between the two experiment types, indicating that the addition of NO_X did not significantly influence the behaviour of non-nitrates upon seed addition. **(c)** same as (a), but in humid conditions (experiment 18, 40 % RH and deliquesced seed). **(d)** the same as (b), but comparing the experiments in (a) and (c): (a) in the y-axis and (c) in the x-axis. The values for fraction remaining for both organonitrates and CHO compounds are consistently lower in the humid case, indicating enhanced uptake in those conditions. In (c) and (d), the y axis has been cut at 1.5 for clarity, excluding the compound $C_5H_6O_6$ at mass 224 with a fraction remaining of 2.27.

(~~Fig~~Figs. 6 (~~b)~~ c) and (d)). It is plausible that this increased uptake of the oxidation products was caused by the formation of an aqueous phase on the particles, and solubility-driven or reactive uptake of the oxidation products to the aqueous phase.

3.6 Factors determining HOM volatility

To gain more insight on what determines the volatility of HOM, we constructed a statistical model explaining their condensation behaviour, measured by the fraction remaining, in terms of their composition. From Fig. 6, it is already clear that the molecular mass of the compounds explains the volatility relatively well, with increasing mass decreasing the volatility. How-

ever, molecular mass cannot explain all the features of the curve, such as the different behaviour of nitrates and non-nitrates. Furthermore, the molecular mass in itself provides no causal explanation for the volatility: rather, low volatility is caused by intermolecular forces: thus, intermolecularly bonding functional groups lower the volatility of a compound (e.g. Kroll and Seinfeld, 2008). These are not directly measured by the mass spectrometric technique, but the composition of a compound gives some indication as to what functional groups it may contain. As an example, a hydroxy group will contribute, in addition to a hydrogen atom, one oxygen, while a hydroperoxide group will contribute two. In contrast, an aldehyde or a ketone group will contribute one oxygen, while reducing the number of hydrogen atoms bound to the carbon skeleton by one. Thus, all of these groups will contribute a different number of hydrogen and oxygen atoms. However, these contributions are not unique, as a compound with two hydroxy groups will have the same composition as that having one ~~hyrdoperoxide~~ hydroperoxide group, everything else being equal. Still, the composition can provide indication of the functionalities of a molecule as well.

3.6.1 ~~Logistic regression~~ Generalized linear model to explain HOM volatility

For the analysis, we chose to use the average of experiments 15 and 19 (Table A1, the same as presented in Fig. 6 (a)), with AS seed injection, dry chamber and with NO_X in the chamber. We chose these experiments in order to minimize the role of particle phase processes in determining the FR, and in order to be able to incorporate organic nitrates into our model. We linearly scaled the fractions remaining (FR) of HOM to range from zero to one, with the upper branch of the sigmoid in Fig. 6 (a) getting the value one, and the lower branch, containing essentially non-volatile HOM dimers, the value zero. We used this scaled response (FR_{scaled}) as the dependent variable, with the carbon, hydrogen, oxygen and nitrogen numbers of a molecule as the independent variables. With the dependent variable ranging from zero to one, and having a sigmoidal transition between the extremes, we chose to use a generalized linear model with a logit link function ~~. For the modeling we chose to use the average of experiments 16 and 19 (Table A1), with NO in the chamber, as in this way we could incorporate organic nitrates into our model.~~ (i.e. the inverse of the logistic function).

Compounds with less than six carbon atoms, or with a signal to noise ratio below ~~four~~ten, were excluded from the model, in order to avoid the smallest fragments and unreliable signals, respectively. In addition, ~~the~~ any compounds with a FR value over 1.1 (meaning a 10 % increase upon seed addition) were excluded due to the influence of particle phase processes on them. The model was weighted with the signal before seed addition, capped to the same value as in Fig. 6, in order to give more weight to the more abundant oxidation products.

We found that the fraction remaining could be well explained using the composition (Fig. 7). ~~The~~ Out of the monomers, the abundant C_{10} compounds are fitted the best, appearing close to the 1:1 line. The compounds deviating from this line mainly have a smaller carbon number; C_9 compounds seem especially problematic for the model. This could be an indication that the dependence of the volatility on e.g. the oxygen number is different for compounds with fewer than 10 carbon atoms. Both organic nitrates and non-nitrates seem to be fitted equally well. The formula for the fit is:

$$\mathrm{logit}(\mathrm{FR}_{\mathrm{scaled}}) = 0.50.55 \times n_{\mathrm{C}} - 0.40.44 \times n_{\mathrm{H}} - 1.11.2 \times n_{\mathrm{O}} + 2.32.5 \times n_{\mathrm{N}} + 8.79.0. \quad (10)$$

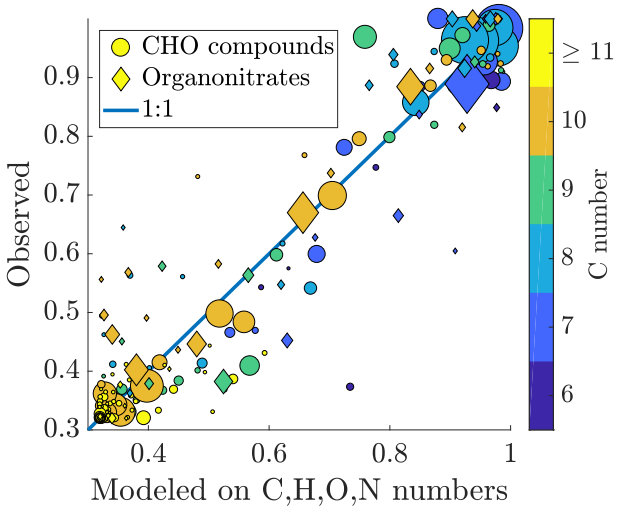

Figure 7. Measured fraction remaining ~~of the y-axis~~ vs. fraction remaining modelled on the chemical composition. The colouring of the circles is based on the carbon number of the compound, and the ~~size~~ area of the circles is scaled ~~according~~ linearly to the signal intensity, as in Figs. 5 and 6. The ~~coefficients~~ formula for the ~~binomial~~ model ~~are~~ is presented in Eq. (10). Number of compounds used for the fit: n = ~~442~~232, Chi^2-statistic vs. constant model: ~~1.81×10^4~~1.74×10^4, p-value = ~~0.~~0 (to machine precision). A good correspondence is found between the measured and fitted values, indicating that the volatility of a compound can be explained well in terms of its molecular formula. Larger deviances from the 1:1 line are mainly explained by carbon numbers lower than ten.

The coefficients for each of the terms in the model, including the intercept, were highly statistically significant, with all p values being smaller than ~~10^{-53}~~10^{-51}. To convert the dependent variable to volatility, we used the logistic fit between the saturation concentration of a model compound, and ~~the~~ its expected fraction remaining from Fig. 3. By combining that relationship with the logistic fit in Eq. (10), we can obtain an expression for the saturation vapour concentration in terms of the composition:

$$\log_{10}(\mathrm{C}^*[\mu\mathrm{g\ m}^{-3}]) = 0.160.18 \times n_\mathrm{C} - 0.130.14 \times n_\mathrm{H} - 0.360.38 \times n_\mathrm{O} + 0.760.80 \times n_\mathrm{N} + 2.83.1. \quad (11)$$

The addition of a carbon or a nitrogen atom to a molecule, with their positive coefficients in the model, would act as to increase the volatility. The addition of a hydrogen or an oxygen atom, on the other hand, would act as to decrease it. The positive coefficients of carbon and nitrogen seem counter-intuitive at first. However, the addition or removal of a carbon or a nitrogen atom is not independent of other elements. In the case of HOM formed here, the nitrogen most probably appears in the form of a nitrate functional group (NO_3), and is thus accompanied by three oxygen atoms. Adding the coefficients of the nitrogen atom with three oxygen results in a negative overall coefficient. The cumulative effect of adding a nitrate group would therefore act to reduce the fraction remaining, and thus volatility, in agreement with widely used group contribution methods, such as SIMPOL developed by Pankow and Asher (2008). Similarly, addition or removal of a carbon atom, while

keeping the structure of the molecule otherwise unchanged, would be accompanied by the corresponding gain or loss of two hydrogen atoms. The combined effect would still be to decrease the volatility with increasing carbon number, as expected. Even accounting for the carbon number in the model, the hydrogen number of a molecule also got a statistically significant coefficient. This indicates that the hydrogen number provides independent information on the volatility of a compound, with the volatility decreasing with increasing hydrogen number. The termination step of an RO_2 radical formed in the ozonolysis of α-pinene determines the number of hydrogen atoms in the resulting molecule, with lower hydrogen numbers being accompanied by the formation of a carbonyl group, and higher numbers accompanied with a hydroxy group (Vereecken and Francisco, 2012). The hydroxy group is expected to lower the volatility of a compound more than the carbonyl group (Kroll and Seinfeld, 2008). Thus, the negative coefficient of hydrogen in our model, as well as the coefficients of other elements, are reasonable in the light of molecular considerations for the determination of volatility.

As before, any compounds with a saturation concentration higher than 100 μg m^{-3} (volatile end of SVOC range) are expected to behave in the same way, not being affected by the seed addition, and showing values for fraction remaining of around one (Fig. 3). Similarly, compounds with a saturation concentration below 0.01 μg m^{-3} (in the LVOC range) are all expected to behave as non-volatile. Thus, the model, similarly to the measured results, cannot distinguish between volatilities of compounds above and below these limits, respectively. From this follows that the model is most reliably fit to the compounds in the transition region, in the SVOC to LVOC range. The relationship given in Eq. (11) may only hold for that range of volatilities. Thus, caution should be used in interpreting the modelled volatilities, especially outside the range of volatilities defined above. E.g. HOM dimers, which all exhibit behaviour consistent with non-volatile vapours, are correctly fit in the very lowest edge of the volatility range, but any detailed information on their volatility is lost. For this reason, the relationship given in Eq. (11) may be better suited for HOM monomers. Also, the relationship presented in Eq. (11) may not hold for oxidation systems other than the one presented here~~. Therefore,~~, or indeed compounds formed in α-pinene oxidation, but not through autoxidation. Examples of products formed in the latter way include pinic ($C_9H_{14}O_4$) and pinonic acids ($C_{10}H_{16}O_3$). Equation (11) gives them saturation concentrations 15 μg m^{-3} and 27 μg m^{-3}, respectively, compared to literature values in the range of a couple of μg m^{-3} for pinic and from less than one to up to hundreds of μg m^{-3} for pinonic acid (Bilde and Pandis, 2001; Salo et al., 2010; Donahue et al., 2012). Especially for pinonic acid the spread in literature values is very large. Given that HOM are chemically quite different from the two acids, the agreement is surprisingly good. Still, any generalizations should be drawn with caution. Finally, the possibility that the uptake of some compounds to particles is not driven by their volatility, but rather some particle phase processes (as noted in Sect. 2.4.4) would affect the modelling as well. This would lead to artificially low volatility estimates. However, as noted above, we have tried to minimize this effect.

3.6.2 Comparison to existing volatility parametrizations

There are numerous existing parametrizations for assessing the volatility of VOC oxidation products. Some, like the SIMPOL model by Pankow and Asher (2008), require as inputs the exact functional groups making up a molecule. Others, such as the ~~one presented in Bianchi et al. (2019) , and the one devised by~~ ones presented by Bianchi et al. (2019) and Tröstl et al. (2016), only require the molecular formula, having some underlying structural assumptions. The former requires the carbon and oxygen

numbers in the molecule. The presence of nitrogen is separately handled, by assuming it to exist in nitrate functional groups, assigning a constant effect to that nitrate group. The latter is based on the estimated SIMPOL volatilities for certain expected model HOM compounds, and fit based on their O:C ratios, separately for C_{10} monomers and C_{20} dimers, with each group getting their own relationship. As the exact structures of HOM are not known (Bianchi et al., 2019), any method requiring structural information, such as SIMPOL, will include some uncertainty stemming from the choice of structure for a compound. Similarly, the SIMPOL-based parametrization by Tröstl et al. (2016), will include this uncertainty.

In the SIMPOL model, any addition of oxygen to the molecule decreases its volatility by almost an order of magnitude, at minimum (for a ketone). A hydroxy or a hydroperoxy group both lower the volatility by over 2 orders of magnitude, as does a nitrate group. In our parametrization (Eq. (11)), the coefficient for ~~one oxygen atom is~~ oxygen is -0.36. This ~~corresponds to a reduction in volatility of only~~ means that with the addition of one oxygen atom, the volatility of a compound is reduced by only a bit more than a factor of ~~2 with the addition of an oxygen atom.~~ 2. Thus, even for a hydroperoxy group, containing two oxygens, the reduction in volatility would be only 5-fold. For a nitrate group, the corresponding decrease in volatility would be a factor of 2. Thus, our parametrization in Eq. (11) seems to predict much smaller sensitivities of the volatility of HOM to different functional groups than what would be expected based on e.g. SIMPOL.

Using quantum chemical calculations by the COSMO-RS model, Kurtén et al. (2016) found that intramolecular hydrogen bonding between the functional groups within a HOM molecule may inhibit the ability of the groups to take part in intermolecular bonding, and thus to reduce the volatility of the molecule. This would lead to the volatility being less sensitive to addition of functional groups than would be expected based on e.g. SIMPOL. As noted above, our results support this lower than expected sensitivity.

As a result of the lower sensitivity of the volatility to additional functional groups, Kurtén et al. (2016) hypothesised that the volatilities of HOM may be higher than expected based on group contribution methods. As a best estimate, they suggested to use the geometric mean of the SIMPOL and COSMO-RS values for the volatility of HOM. Additionally, Kurtén et al. (2016) found that for the same molecular formula, the volatility estimates by both the group contribution methods and by the COSMO-RS model varied up to 4 orders of magnitude depending one the exact structure chosen. To compare our results to those presented by Kurtén et al. (2016), as well as the parametrizations by Bianchi et al. (2019) and Tröstl et al. (2016), we took a set of model HOM compounds from Kurtén et al. (2016), and calculated the volatility estimates for them using both those parametrizations, as well as using Eq. (11).

For $C_{10}H_{16}O_X$, with X ranging from 6 to 10, we found that our parametrization generally gives lower volatilities than the geometric mean of COSMO-RS and SIMPOL estimates, especially for the higher oxygen numbers (~~Table ??~~Fig. 8). However, as noted above, both of those methods show a large variability depending on the exact structure of the molecule. ~~However, compared~~ Compared to the parametrizations by Bianchi et al. (2019) and Tröstl et al. (2016), and the lower end of SIMPOL estimates, our parametrization generally gives higher volatilities. Further, as noted above, our parametrization is much less sensitive to the addition of oxygen as compared to either Bianchi et al. (2019) or Tröstl et al. (2016). In this aspect, our parametrization is closer to COSMO-RS. However, the actual volatility estimates in our parametrization are much lower than those given by COSMO-RS. Our results thus fit in with the existing literature, in that the volatility of HOM seems to be less

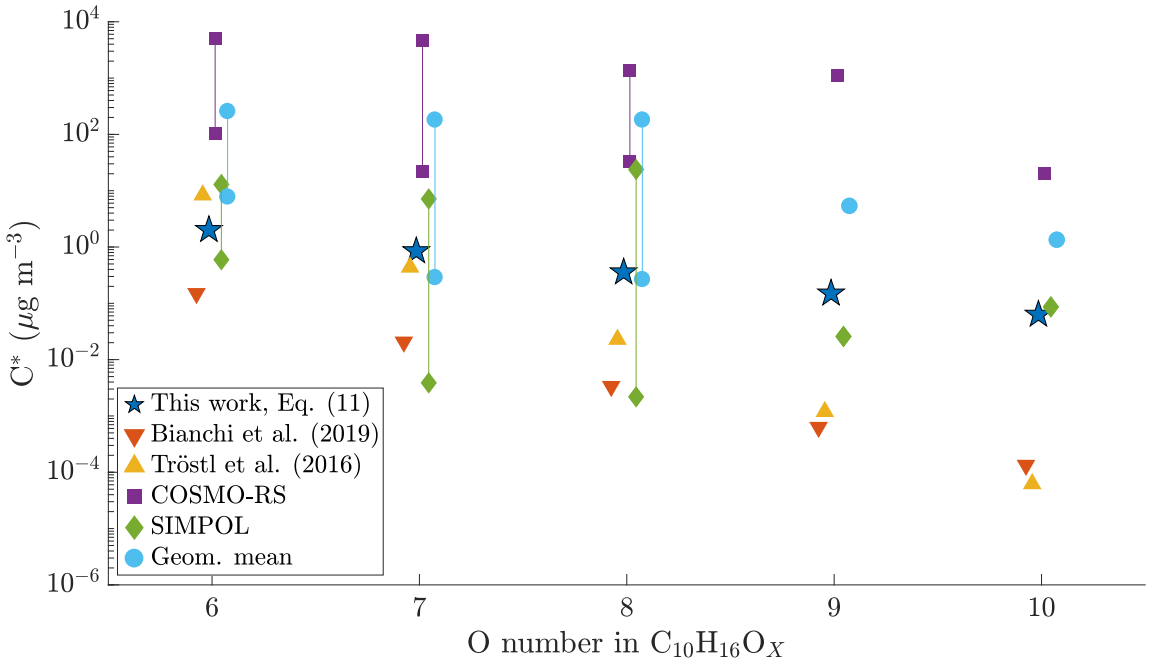

Figure 8. Comparison of different volatility estimates and parametrizations. SIMPOL and COSMO-RS are from Kurtén et al. (2016): COSMO-RS is the geometric mean of their four different COSMO-RS estimates. Geom. mean is the geometric mean of SIMPOL and COSMO-RS as recommended by Kurtén et al. (2016). For compounds with six to eight oxygen atoms, Kurtén et al. (2016) used multiple candidate isomers: values are given ~~separately~~ both for the one with the highest ~~(subscript h)~~ and the lowest ~~(subscript l)~~ saturation concentration. For the parametrizations from Tröstl et al. (2016), Bianchi et al. (2019) and Eq. (11), all structural isomers get the same value, and thus only one is given. All values are saturation vapour concentrations in μg m^{-3}. The values from Kurtén et al. (2016) are calculated at 298.15 K, Tröstl et al. (2016) at 293 K, Bianchi et al. (2019) at 300 K and Eq. (11) at chamber temperature, approx. 302 K.

sensitive to oxygen addition than expected from SIMPOL, as suggested by Kurtén et al. (2016). However, the absolute values of the volatility seem to be lower than those suggested by Kurtén et al. (2016) but still higher than from Bianchi et al. (2019). ~~Also~~Again, as noted above, we cannot fully exclude the role of particle phase processes in artificially lowering our HOM volatility estimates.

~~molecule SIMPOL COSMO-RS Geom. mean Tröstl et al. (2016) Bianchi et al. (2019) Eq. (11) $C_{10}H_{16}O_6$ $_h$1.3×10^1 $_h$5.1×10^3 $_h$2.6×10^2 8.3×10^0 1.5×10^{-1} 1.4×10^0 $_l$6.0×10^{-1} $_l$1.0×10^2 $_l$7.8×10^0 $C_{10}H_{16}O_7$ $_h$7.2×10^0 $_h$4.6×10^3 $_h$1.8×10^2 4.4×10^{-1} 2.0×10^{-2} 6.3×10^{-1} $_l$3.9×10^{-3} $_l$2.2×10^1 $_l$2.9×10^{-1} $C_{10}H_{16}O_8$ $_h$2.4×10^1 $_h$1.4×10^3 $_h$3.1×10^1 2.2×10^{-2} 3.2×10^{-3} 2.8×10^{-1} $_l$2.2×10^{-3} $_l$3.3×10^1 $_l$2.7×10^{-1} $C_{10}H_{16}O_9$ 2.6×10^{-2} 1.1×10^3 5.4×10^0 1.2×10^{-3} 6.3×10^{-4} 1.2×10^{-1} $C_{10}H_{16}O_{10}$ 8.7×10^{-2} 2.1×10^1 1.3×10^0 6.3×10^{-5} 1.3×10^{-4} 5.2×10^{-2}~~

4 Conclusions

To investigate the volatility of HOM formed in the ozonolysis of the monoterpene α-pinene, we used injections of inorganic seed aerosol to promote their condensation in a continuous flow chamber experiment. We found that, as expected, the general trend was that the higher the mass of the oxidation product, the more their gas phase signal dropped during the seed injections, down to levels consistent with irreversible condensation. The observed changes were consistent with the lowering of the volatility of the compounds with increasing mass. The most highly oxidized HOM monomers, along with HOM dimers, were determined to be of low or extremely low volatility. Compared to non-nitrate oxidation products, we found that organic nitrates of comparable volatility had a higher mass, probably due to the relatively high mass of the nitrate group. The type of seed (ammonium sulfate, or the more acidic ammonium bisulfate) did not have a notable effect on the condensation behaviour of HOM, while in a humid chamber the uptake of ~~some~~ many compounds was observed to be higher.

We found that the behaviour of the compounds upon seed injection, and thus their volatility, could be well explained in terms of their chemical composition. We found carbon, hydrogen, oxygen and nitrogen numbers all to be important in explaining the volatility, and the relationship could be connected to molecular properties of the compounds. Based on this relationship, we were able to develop a parametrization for the volatility of HOM monomers generated in α-pinene ozonolysis. ~~In future studies , this parametrization should be used to further clarify the role of HOM in~~ Future studies should evaluate the effect of the exact volatility parametrization used on new particle formation from HOM.

The results presented here are possibly specific to HOM from the ozonolysis of α-pinene, but the general methodology should be applicable to other conditions as well. These conditions may include other oxidant-VOC-combinations, but also different loadings of organic aerosol to probe different volatility ranges. However, in investigations of volatility, care should be taken to affirm that the observed changes in gas phase signals are in fact caused by volatility, and not changes in gas phase chemistry, for example.

Code and data availability. Data will be available from a persistent repository and upon request from corresponding authors. Codes for the analysis will be available from OP, and the ADCHAM model code is available from PR upon request.

Appendix A

A1

Author contributions. Conceptualization: OP, MR, ME; Formal analysis: OP (lead), PR (supporting); Funding acquisition: OP, ME; Investigation: OP, MR, LH, LQ, ME; Methodology: OP, MR, PR, ME; Software: PR; Supervision: ME; Validation: OP; Visualization: OP; Writing - original draft: OP; Writing - review & editing: All coauthors.

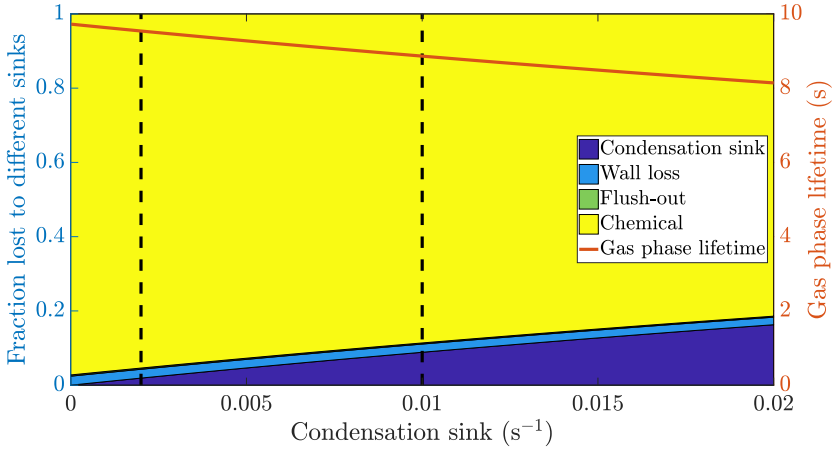

Figure A1. The calculated fraction of RO_2 radicals lost to different sinks, and their total lifetime in the gas phase as a function of the condensation sink caused by aerosol particles in the chamber. The chemical lifetime of RO_2 is estimated to be 10 seconds, and the wall loss lifetime 400 seconds. The vertical broken lines at 0.002 s^{-1} and 0.01 s^{-1} represent a typical situation without seed particles and with seed particles, respectively.

Competing interests. The authors declare that they have no competing interests.

Acknowledgements. We would like to thank Olga Garmash and Chao Yan for helpful discussions, and Simon Schallhart for help in interpreting the PTR-TOF data. This work was funded by the European Research Council (ERC-StG 638703-COALA), the Academy of Finland (Project numbers 317380 and 320094), the Vilho, Yrjö and Kalle Väisälä Foundation and the Swedish Research Council Formas (Project no. 2018-1745). We thank the TofTools team for providing tools for mass spectrometry data analysis.

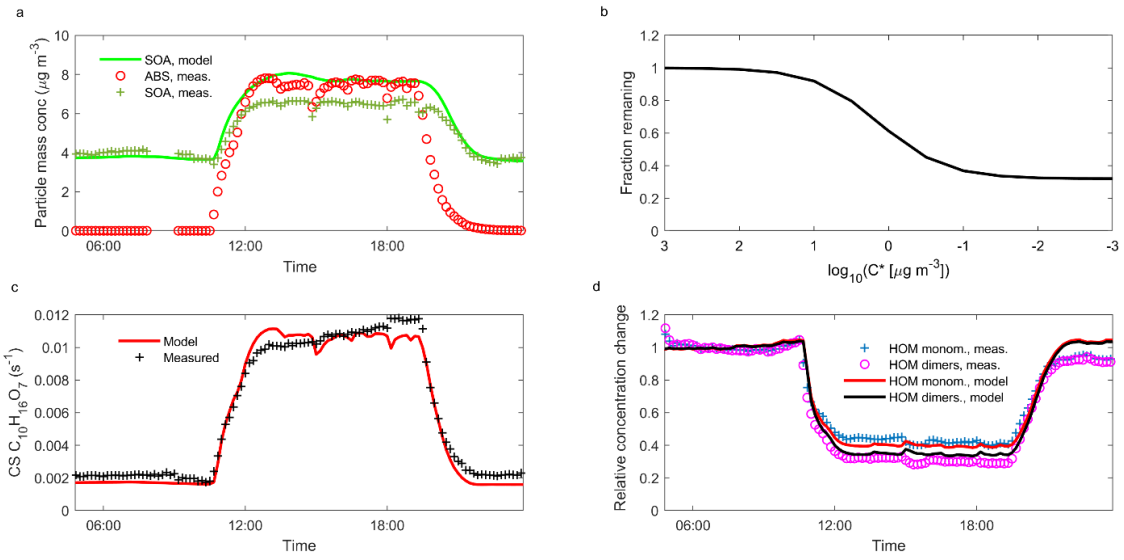

Figure A2. Experiment ~~4~~ 3 modeled with ADCHAM. a: the measured and modelled ABS and organic aerosol concentrations. b: the modelled fraction remaining as a function of saturation vapour concentration. c: modelled and measured CS for a compound with molecular formula $C_{10}H_{16}O_7$. d: modelled and measured relative change in the concentration of HOM monomers and dimers. The measured HOM monomers and dimer are represented by the total concentration of molecules in the mass range 290-450 Da and 452-600 Da (including the NO_3^- ion).

References

Aalto, P., Hämeri, K., Becker, E., Weber, R., Salm, J., Mäkelä, J., Hoell, C., O'Dowd, C., Karlsson, H., Hansson, H., Väkevä, M., Koponen, I., Buzorius, G., and Kulmala, M.: Physical characterization of aerosol particles during nucleation events, Tellus Series B-Chemical And Physical Meteorology, 53, 344–358, https://doi.org/10.1034/j.1600-0889.2001.530403.x, 2001.

Atkinson, R., Aschmann, S. M., Arey, J., and Shorees, B.: Formation of OH radicals in the gas phase reactions of O3 with a series of terpenes, Journal of Geophysical Research: Atmospheres, 97, 6065–6073, https://doi.org/10.1029/92JD00062, 1992.

Berndt, T., Mentler, B., Scholz, W., Fischer, L., Herrmann, H., Kulmala, M., and Hansel, A.: Accretion Product Formation from Ozonolysis and OH Radical Reaction of α-Pinene: Mechanistic Insight and the Influence of Isoprene and Ethylene, Environmental Science & Technology, 52, 11 069–11 077, https://doi.org/10.1021/acs.est.8b02210, 2018a.

Berndt, T., Scholz, W., Mentler, B., Fischer, L., Herrmann, H., Kulmala, M., and Hansel, A.: Accretion Product Formation from Self- and Cross-Reactions of RO_2 Radicals in the Atmosphere, Angewandte Chemie Int Ed, https://doi.org/10.1002/anie.201710989, 2018b.

Bianchi, F., Tröstl, J., Junninen, H., Frege, C., Henne, S., Hoyle, C. R., Molteni, U., Herrmann, E., Adamov, A., Bukowiecki, N., Chen, X., Duplissy, J., Gysel, M., Hutterli, M., Kangasluoma, J., Kontkanen, J., Kürten, A., Manninen, H. E., Münch, S., Peräkylä, O., Petäjä, T., Rondo, L., Williamson, C., Weingartner, E., Curtius, J., Worsnop, D. R., Kulmala, M., Dommen, J., and Baltensperger, U.: New particle formation in the free troposphere: A question of chemistry and timing, Science, 352, 1109–1112, https://doi.org/10.1126/science.aad5456, http://science.sciencemag.org/content/352/6289/1109, 2016.

Table A1. Overview of experimental conditions. AS = ammonium sulfate, ABS = ammonium bisulfate, eff = effloresced seed, deli = deliquesced seed. Condensation sinks are calculated for $C_{10}H_{16}O_7$ from the dry size distribution, and listed separately for the steady states before (SS_1) and during (SS_2) seed injection. For the beginning of Experiment ~~7~~6, the DMPS was malfunctioning and CS is thus not given.

#	T (K)	RH (%)	[AP] (ppb)	[O_3] (ppb)	[NO_X] (ppb)	[NO] (ppt)	Seed	Seed state	CS_{SS_1} (s^{-1})	CS_{SS_2} (s^{-1})
~~2~~ 1	302	<1	33	70	0	0	AS	eff	0.90×10^{-3}	9.0×10^{-3}
~~3~~ 2	302	44	22	79	0	0	AS	eff	1.0×10^{-3}	15×10^{-3}
~~4~~ 3	303	40	22	80	0	0	ABS	eff	2.1×10^{-3}	11×10^{-3}
~~5~~ 4	303	44	21	78	0	0	ABS	deli	2.4×10^{-3}	12×10^{-3}
~~6~~ 5	302	47	22	79	0	0	AS	deli	2.1×10^{-3}	14×10^{-3}
~~7~~ 6	302	45	23	79	0	0	ABS	deli	NA	8.8×10^{-3}
~~8~~ 7	302	45	22	78	0	0	AS	eff	1.6×10^{-3}	10×10^{-3}
~~9~~ 8	302	42	23	78	0	0	AS	eff	1.5×10^{-3}	12×10^{-3}
~~10~~ 9	303	45	21	77	0	0	ABS	eff	2.2×10^{-3}	8.5×10^{-3}
~~11~~ 10	301	47	35	75	0	0	AS	eff	1.5×10^{-3}	5.6×10^{-3}
~~12~~ 11	300	<1	35	82	0	0	AS	eff	2.4×10^{-3}	8.6×10^{-3}
~~13~~ 12	301	<1	34	75	0	0	ABS	eff	2.2×10^{-3}	9.3×10^{-3}
~~14~~ 13	301	<1	35	66	0	0	ABS	eff	2.2×10^{-3}	9.9×10^{-3}
~~15~~ 14	302	46	24	73	0	0	ABS	deli	3.0×10^{-3}	7.7×10^{-3}
~~16~~ 15	302	<1	91	40	33	110	AS	eff	1.2×10^{-3}	9.5×10^{-3}
~~21~~ 16	302	46	61	40	25	120	ABS	deli	0.73×10^{-3}	7.5×10^{-3}
17	302	42	59	48	25	200	ABS	deli	1.1×10^{-3}	7.9×10^{-3}
18	301	43	60	47	25	200	AS	deli	1.1×10^{-3}	9.1×10^{-3}
19	302	<1	86	51	33	180	AS	eff	1.0×10^{-3}	9.1×10^{-3}
20	302	<1	85	48	33	180	ABS	eff	1.2×10^{-3}	12×10^{-3}

Bianchi, F., Kurtén, T., Riva, M., Mohr, C., Rissanen, M. P., Roldin, P., Berndt, T., Crounse, J. D., Wennberg, P. O., Mentel, T. F., Wildt, J., Junninen, H., Jokinen, T., Kulmala, M., Worsnop, D. R., Thornton, J. A., Donahue, N., Kjaergaard, H. G., and Ehn, M.: Highly Oxygenated Organic Molecules (HOM) from Gas-Phase Autoxidation Involving Peroxy Radicals: A Key Contributor to Atmospheric Aerosol, Chem. Rev., https://doi.org/10.1021/acs.chemrev.8b00395, 2019.

Bilde, M. and Pandis, S. N.: Evaporation Rates and Vapor Pressures of Individual Aerosol Species Formed in the Atmospheric Oxidation of α- and β-Pinene, Environmental Science & Technology, 35, 3344–3349, https://doi.org/10.1021/es001946b, pMID: 11529575, 2001.

Crounse, J. D., Nielsen, L. B., Jørgensen, S., Kjaergaard, H. G., and Wennberg, P. O.: Autoxidation of organic compounds in the atmosphere, The Journal of Physical Chemistry Letters, 4, 3513–3520, https://doi.org/10.1021/jz4019207, http://dx.doi.org/10.1021/jz4019207, 2013.

Cubison, M. and Jimenez, J.: Statistical precision of the intensities retrieved from constrained fitting of overlapping peaks in high-resolution mass spectra, Atmos Meas Tech, 8, 2333–2345, https://doi.org/10.5194/amt-8-2333-2015, 2015.

Dal Maso, M., Kulmala, M., Riipinen, I., Wagner, R., Hussein, T., Aalto, P., and Lehtinen, K.: Formation and growth of fresh atmospheric aerosols: eight years of aerosol size distribution data from SMEAR II, Hyytiala, Finland, BOREAL ENVIRONMENT RESEARCH, 10, 323–336, 2005.

DeCarlo, P. F., Kimmel, J. R., Trimborn, A., Northway, M. J., Jayne, J. T., Aiken, A. C., Gonin, M., Fuhrer, K., Horvath, T., Docherty, K. S., Worsnop, D. R., and Jimenez, J. L.: Field-Deployable, High-Resolution, Time-of-Flight Aerosol Mass Spectrometer, Analytical Chemistry, 78, 8281–8289, https://doi.org/10.1021/ac061249n, 2006.

Donahue, N. M., Kroll, J. H., Pandis, S. N., and Robinson, A. L.: A two-dimensional volatility basis set – Part 2: Diagnostics of organic-aerosol evolution, Atmospheric Chemistry and Physics, 12, 615–634, https://doi.org/10.5194/acp-12-615-2012, http://www.atmos-chem-phys.net/12/615/2012/, 2012.

Ehn, M., Berndt, T., Wildt, J., and Mentel, T.: Highly Oxygenated Molecules from Atmospheric Autoxidation of Hydrocarbons: A Prominent Challenge for Chemical Kinetics Studies, Int J Chem Kinet, 49, 821–831, https://doi.org/10.1002/kin.21130, 2017.

Ehn, M., Thornton, J. A., Kleist, E., Sipilä, M., Junninen, H., Pullinen, I., Springer, M., Rubach, F., Tillmann, R., Lee, B., Lopez-Hilfiker, F., Andres, S., Acir, I.-H., Rissanen, M., Jokinen, T., Schobesberger, S., Kangasluoma, J., Kontkanen, J., Nieminen, T., Kurtén, T., Nielsen, L. B., Jørgensen, S., Kjaergaard, H. G., Canagaratna, M., Dal Maso, M., Berndt, T., Petäjä, T., Wahner, A., Kerminen, V.-M., Kulmala, M., Worsnop, D. R., Wildt, J., and Mentel, T. F.: A large source of low-volatility secondary organic aerosol, Nature, 506, 476–479, https://doi.org/10.1038/nature13032, 2014.

Garmash, O., Rissanen, M. P., Pullinen, I., Schmitt, S., Kausiala, O., Tillmann, R., Percival, C., Bannan, T. J., Priestley, M., Hallquist, Å. M., Kleist, E., Kiendler-Scharr, A., Hallquist, M., Berndt, T., McFiggans, G., Wildt, J., Mentel, T., and Ehn, M.: Multi-generation OH oxidation as a source for highly oxygenated organic molecules from aromatics, Atmospheric Chemistry and Physics Discussions, 2019, 1–33, https://doi.org/10.5194/acp-2019-582, 2019.

Graus, M., Müller, M., and Hansel, A.: High Resolution PTR-TOF: Quantification and Formula Confirmation of VOC in Real Time, Journal of the American Society for Mass Spectrometry, 21, 1037 – 1044, https://doi.org/10.1016/j.jasms.2010.02.006, http://www.sciencedirect.com/science/article/pii/S1044030510001005, 2010.

Hallquist, M., Wenger, J. C., Baltensperger, U., Rudich, Y., Simpson, D., Claeys, M., Dommen, J., Donahue, N. M., George, C., Goldstein, A. H., Hamilton, J. F., Herrmann, H., Hoffmann, T., Iinuma, Y., Jang, M., Jenkin, M. E., Jimenez, J. L., Kiendler-Scharr, A., Maenhaut, W., McFiggans, G., Mentel, T. F., Monod, A., Prévôt, A. S. H., Seinfeld, J. H., Surratt, J. D., Szmigielski, R., and Wildt, J.: The formation, properties and impact of secondary organic aerosol: current and emerging issues, Atmospheric Chemistry and Physics, 9, 5155–5236, https://doi.org/10.5194/acp-9-5155-2009, http://www.atmos-chem-phys.net/9/5155/2009/, 2009.

Jenkin, M. E., Saunders, S. M., and Pilling, M. J.: The tropospheric degradation of volatile organic compounds: a protocol for mechanism development, Atmospheric Environment, 31, 81 – 104, https://doi.org/10.1016/S1352-2310(96)00105-7, 1997.

Jimenez, J., Canagaratna, M., Donahue, N., Prevot, A., Zhang, Q., Kroll, J., P., D., Allan, J., Coe, H., Ng, N., Aiken, A., Docherty, K., Ulbrich, I., Grieshop, A., Robinson, A., Duplissy, J., Smith, J., Wilson, K., Lanz, V., Hueglin, C., Sun, Y., Tian, J., Laaksonen, A., Raatikainen, T., Rautiainen, J., Vaattovaara, P., Ehn, M., Kulmala, M., Tomlinson, J., Collins, D., Cubison, M., E., E., Dunlea, J., Huffman, J., Onasch, T., Alfarra, M., Williams, P., Bower, K., Kondo, Y., Schneider, J., Drewnick, F., Borrmann, S., Weimer, S., Demerjian, K., Salcedo, D., Cottrell, L., Griffin, R., Takami, A., Miyoshi, T., Hatakeyama, S., Shimono, A., Sun, J., Zhang, Y., Dzepina, K., Kimmel, J., Sueper, D., Jayne, J., Herndon, S., Trimborn, A., Williams, L., Wood, E., Middlebrook, A., Kolb, C., Baltensperger, U., and Worsnop, D.: Evolution of Organic Aerosols in the Atmosphere, Science, 326, 1525–1529, https://doi.org/10.1126/science.1180353, 2009.

Jokinen, T., Sipilä, M., Junninen, H., Ehn, M., Lönn, G., Hakala, J., Petäjä, T., Mauldin III, R. L., Kulmala, M., and Worsnop, D. R.: Atmospheric sulphuric acid and neutral cluster measurements using CI-APi-TOF, Atmospheric Chemistry and Physics, 12, 4117–4125, https://doi.org/10.5194/acp-12-4117-2012, http://www.atmos-chem-phys.net/12/4117/2012/, 2012.

Jokinen, T., Sipilä, M., Richters, S., Kerminen, V.-M., Paasonen, P., Stratmann, F., Worsnop, D., Kulmala, M., Ehn, M., Herrmann, H., and Berndt, T.: Rapid autoxidation forms highly oxidized RO_2 radicals in the atmosphere, Angewandte Chemie International Edition, 53, 14 596–14 600, https://doi.org/10.1002/anie.201408566, 2014.

Junninen, H., Ehn, M., Petäjä, T., Luosujärvi, L., Kotiaho, T., Kostiainen, R., Rohner, U., Gonin, M., Fuhrer, K., Kulmala, M., and Worsnop, D. R.: A high-resolution mass spectrometer to measure atmospheric ion composition, Atmospheric Measurement Techniques, 3, 1039–1053, https://doi.org/10.5194/amt-3-1039-2010, http://www.atmos-meas-tech.net/3/1039/2010/, 2010.

Kirkby, J., Duplissy, J., Sengupta, K., Frege, C., Gordon, H., Williamson, C., Heinritzi, M., Simon, M., Yan, C., Almeida, J., Tröstl, J., Nieminen, T., Ortega, I. K., Wagner, R., Adamov, A., Amorim, A., Bernhammer, A.-K., Bianchi, F., Breitenlechner, M., Brilke, S., Chen, X., Craven, J., Dias, A., Ehrhart, S., Flagan, R. C., Franchin, A., Fuchs, C., Guida, R., Hakala, J., Hoyle, C. R., Jokinen, T., Junninen, H., Kangasluoma, J., Kim, J., Krapf, M., Kürten, A., Laaksonen, A., Lehtipalo, K., Makhmutov, V., Mathot, S., Molteni, U., Onnela, A., Peräkylä, O., Piel, F., Petäjä, T., Praplan, A. P., Pringle, K., Rap, A., Richards, N. A. D., Riipinen, I., Rissanen, M. P., Rondo, L., Sarnela, N., Schobesberger, S., Scott, C. E., Seinfeld, J. H., Sipilä, M., Steiner, G., Stozhkov, Y., Stratmann, F., Tomé, A., Virtanen, A., Vogel, A. L., Wagner, A. C., Wagner, P. E., Weingartner, E., Wimmer, D., Winkler, P. M., Ye, P., Zhang, X., Hansel, A., Dommen, J., Donahue, N. M., Worsnop, D. R., Baltensperger, U., Kulmala, M., Carslaw, K. S., and Curtius, J.: Ion-induced nucleation of pure biogenic particles, Nature, 533, 521–526, http://dx.doi.org/10.1038/nature17953, letter, 2016.

Krechmer, J., Pagonis, D., Ziemann, P., and Jimenez, J.: Quantification of Gas-Wall Partitioning in Teflon Environmental Chambers Using Rapid Bursts of Low-Volatility Oxidized Species Generated in Situ, Environ Sci Technol, 50, 5757–5765, https://doi.org/10.1021/acs.est.6b00606, 2016.

Kroll, J. H. and Seinfeld, J. H.: Chemistry of secondary organic aerosol: Formation and evolution of low-volatility organics in the atmosphere, Atmospheric Environment, 42, 3593 – 3624, https://doi.org/10.1016/j.atmosenv.2008.01.003, http://www.sciencedirect.com/science/article/pii/S1352231008000253, 2008.

Kurtén, T., Tiusanen, K., Roldin, P., Rissanen, M., Luy, J., Boy, M., Ehn, M., and Donahue, N.: α-Pinene Autoxidation Products May Not Have Extremely Low Saturation Vapor Pressures Despite High O:C Ratios, J Phys Chem, 120, 2569–2582, https://doi.org/10.1021/acs.jpca.6b02196, 2016.

Matsunaga, A. and Ziemann, P. J.: Gas-Wall Partitioning of Organic Compounds in a Teflon Film Chamber and Potential Effects on Reaction Product and Aerosol Yield Measurements, Aerosol Science and Technology, 44, 881–892, https://doi.org/10.1080/02786826.2010.501044, 2010.

Mentel, T. F., Springer, M., Ehn, M., Kleist, E., Pullinen, I., Kurtén, T., Rissanen, M., Wahner, A., and Wildt, J.: Formation of highly oxidized multifunctional compounds: autoxidation of peroxy radicals formed in the ozonolysis of alkenes – deduced from structure–product relationships, Atmospheric Chemistry and Physics, 15, 6745–6765, https://doi.org/10.5194/acp-15-6745-2015, http://www.atmos-chem-phys.net/15/6745/2015/, 2015.

Pankow, J. F. and Asher, W. E.: SIMPOL.1: a simple group contribution method for predicting vapor pressures and enthalpies of vaporization of multifunctional organic compounds, Atmospheric Chemistry and Physics, 8, 2773–2796, https://doi.org/10.5194/acp-8-2773-2008, https://www.atmos-chem-phys.net/8/2773/2008/, 2008.

Paulson, S. E. and Orlando, J. J.: The reactions of ozone with alkenes: An important source of HOx in the boundary layer, Geophysical Research Letters, 23, 3727–3730, https://doi.org/10.1029/96GL03477, 1996.

Riva, M., Heikkinen, L., Bell, D., Peräkylä, O., Zha, Q., Schallhart, S., Rissanen, M., Imre, D., Petäjä, T., Thornton, J., Zelenyuk, A., and Ehn, M.: Chemical transformations in monoterpene-derived organic aerosol enhanced by inorganic composition, Npj Clim Atmospheric Sci, 2, 2, https://doi.org/10.1038/s41612-018-0058-0, 2019.

Roldin, P., Eriksson, A. C., Nordin, E. Z., Hermansson, E., Mogensen, D., Rusanen, A., Boy, M., Swietlicki, E., Svenningsson, B., Zelenyuk, A., and Pagels, J.: Modelling non-equilibrium secondary organic aerosol formation and evaporation with the aerosol dynamics, gas- and particle-phase chemistry kinetic multilayer model ADCHAM, Atmospheric Chemistry and Physics, 14, 7953–7993, https://doi.org/10.5194/acp-14-7953-2014, 2014.

Roldin, P., Ehn, M., Kurtén, T., Olenius, T., Rissanen, M. P., Sarnela, N., Elm, J., Rantala, P., Hao, L., Hyttinen, N., Heikkinen, L., Worsnop, D. R., Pichelstorfer, L., Xavier, C., Clusius, P., Öström, E., Petäjä, T., Kulmala, M., Vehkamäki, H., Virtanen, A., Riipinen, I., and Boy, M.: The role of highly oxygenated organic molecules in the Boreal aerosol-cloud-climate system, Nature Communications, 10, 4370, https://doi.org/10.1038/s41467-019-12338-8, 2019.

Salo, K., Jonsson, Å. M., Andersson, P. U., and Hallquist, M.: Aerosol Volatility and Enthalpy of Sublimation of Carboxylic Acids, The Journal of Physical Chemistry A, 114, 4586–4594, https://doi.org/10.1021/jp910105h, pMID: 20235543, 2010.

Saunders, S., Jenkin, M., Derwent, R., and Pilling, M.: Protocol for the development of the Master Chemical Mechanism, MCM v3 (Part A): tropospheric degradation of non-aromatic volatile organic compounds, Atmospheric Chemistry and Physics, 3, 161–180, https://doi.org/10.5194/acp-3-161-2003, 2003.

Shrivastava, M., Cappa, C. D., Fan, J., Goldstein, A. H., Guenther, A. B., Jimenez, J. L., Kuang, C., Laskin, A., Martin, S. T., Ng, N. L., Petäjä, T., Pierce, J. R., Rasch, P. J., Roldin, P., Seinfeld, J. H., Shilling, J., Smith, J. N., Thornton, J. A., Volkamer, R., Wang, J., Worsnop, D. R., Zaveri, R. A., Zelenyuk, A., and Zhang, Q.: Recent advances in understanding secondary organic aerosol: Implications for global climate forcing, Reviews of Geophysics, 55, 509–559, https://doi.org/10.1002/2016RG000540, 2017.

Tang, M. J., Shiraiwa, M., Pöschl, U., Cox, R. A., and Kalberer, M.: Compilation and evaluation of gas phase diffusion coefficients of reactive trace gases in the atmosphere: Volume 2. Diffusivities of organic compounds, pressure-normalised mean free paths, and average Knudsen numbers for gas uptake calculations, Atmospheric Chemistry and Physics, 15, 5585–5598, https://doi.org/10.5194/acp-15-5585-2015, 2015.

Tröstl, J., Chuang, W. K., Gordon, H., Heinritzi, M., Yan, C., Molteni, U., Ahlm, L., Frege, C., Bianchi, F., Wagner, R., Simon, M., Lehtipalo, K., Williamson, C., Craven, J. S., Duplissy, J., Adamov, A., Almeida, J., Bernhammer, A.-K., Breitenlechner, M., Brilke, S., Dias, A., Ehrhart, S., Flagan, R. C., Franchin, A., Fuchs, C., Guida, R., Gysel, M., Hansel, A., Hoyle, C. R., Jokinen, T., Junninen, H., Kangasluoma, J., Keskinen, H., Kim, J., Krapf, M., Kürten, A., Laaksonen, A., Lawler, M., Leiminger, M., Mathot, S., Möhler, O., Nieminen, T., Onnela, A., Petäjä, T., Piel, F. M., Miettinen, P., Rissanen, M. P., Rondo, L., Sarnela, N., Schobesberger, S., Sengupta, K., Sipilä, M., Smith, J. N., Steiner, G., Tomè, A., Virtanen, A., Wagner, A. C., Weingartner, E., Wimmer, D., Winkler, P. M., Ye, P., Carslaw, K. S., Curtius, J., Dommen, J., Kirkby, J., Kulmala, M., Riipinen, I., Worsnop, D. R., Donahue, N. M., and Baltensperger, U.: The role of low-volatility organic compounds in initial particle growth in the atmosphere, Nature, 533, 527–531, https://doi.org/10.1038/nature18271, 2016.

Vereecken, L. and Francisco, J.: Theoretical studies of atmospheric reaction mechanisms in the troposphere, Chemical Society Reviews, 41, 6259–6293, https://doi.org/10.1039/c2cs35070j, 2012.

Yan, C., Nie, W., Äijälä, M., Rissanen, M. P., Canagaratna, M. R., Massoli, P., Junninen, H., Jokinen, T., Sarnela, N., Häme, S. A., Schobesberger, S., Canonaco, F., Yao, L., Prévôt, A. S., Petäjä, T., Kulmala, M., Sipilä, M., Worsnop, D. R., and Ehn, M.: Source characterization

of highly oxidized multifunctional compounds in a boreal forest environment using positive matrix factorization, Atmospheric Chemistry and Physics, 16, 12 715–12 731, https://doi.org/10.5194/acp-16-12715-2016, 2016.

Zhang, Q., Jimenez, J. L., Canagaratna, M. R., Allan, J. D., Coe, H., Ulbrich, I., Alfarra, M. R., Takami, A., Middlebrook, A. M., Sun, Y. L., Dzepina, K., Dunlea, E., Docherty, K., DeCarlo, P. F., Salcedo, D., Onasch, T., Jayne, J. T., Miyoshi, T., Shimono, A., Hatakeyama, S., Takegawa, N., Kondo, Y., Schneider, J., Drewnick, F., Borrmann, S., Weimer, S., Demerjian, K., Williams, P., Bower, K., Bahreini, R., Cottrell, L., Griffin, R. J., Rautiainen, J., Sun, J. Y., Zhang, Y. M., and Worsnop, D. R.: Ubiquity and dominance of oxygenated species in organic aerosols in anthropogenically-influenced Northern Hemisphere midlatitudes, Geophysical Research Letters, 34, https://doi.org/10.1029/2007GL029979, l13801, 2007.